Panthalassan seamount-associated Permian-Triassic boundary siliceous rocks, Mino Terrane, Central Japan

Sano, Hiroyoshi
Department of Earth and Planetary Sciences, Kyushu University

Kuwahara, Kiyokoi
Faculty of Clinical Education, Ashiya University

Yao, Akira
Department of Geosciences, Osaka City University

Agematsu, Sachiko
Graduate School of Life and Environmental Sciences, University of Tsukuba

出版情報：Paleontological Research. 14 (4), pp.293-314, 2010-12-31. 日本古生物学会
バージョン：

Panthalassan Seamount-Associated Permian-Triassic Boundary Siliceous Rocks, Mino Terrane, Central Japan

Author(s): Hiroyoshi Sano, Kiyoko Kuwahara, Akira Yao and Sachiko Agematsu
Source: Paleontological Research, 14(4):293-314. 2010.
Published By: The Palaeontological Society of Japan
DOI: 10.2517/1342-8144-14.4.293
URL: http://www.bioone.org/doi/full/10.2517/1342-8144-14.4.293

Paleontological Research, vol. 14, no. 4, pp. 293–314, December 31, 2010

doi:10.2517/1342-8144-14.4.293

Panthalassan seamount-associated Permian-Triassic boundary siliceous rocks, Mino terrane, central Japan

HIROYOSHI SANO[1], KIYOKO KUWAHARA[2], AKIRA YAO[3] AND SACHIKO AGEMATSU[4]

[1]*Department of Earth and Planetary Sciences, Kyushu University, Fukuoka 812-8581, Japan (e-mail: sano@geo.kyushu-u.ac.jp)*
[2]*Faculty of Clinical Education, Ashiya University, Rokurokuso-cho, Ashiya 659-8511, Japan*
[3]*Department of Geosciences, Osaka City University, Osaka 558-8585, Japan*
[4]*Graduate School of Life and Environmental Sciences, University of Tsukuba, Ibaraki 305-8572, Japan*

Received September 15, 2010; Revised manuscript accepted November 11, 2010

Abstract. We describe the lithology and age of an intact section (NF 1212R) and two reference sections of Panthalassan seamount-associated Permian-Triassic boundary (PTB) siliceous rocks. The sections occupy the upper part of the Hashikadani Formation of the Mino terrane in the Mt. Funabuseyama area, central Japan. Section NF 1212R comprises a lower unit of gray chert (ca. 1.7 m thick), a middle unit of dark gray to black chert (ca. 0.8 m) with a pyrite-rich layer at the top (ca. 0.1 m), and an upper unit of black claystone with thin, intermittent beds of black to dark gray chert (ca. 1.2 m), in ascending order. The chert of the lower and middle units is rich in radiolarian remains with minor siliceous sponge spicules. The black chert of the middle unit is carbonaceous and includes tiny pyrite grains. The black claystone consists of microcrystalline quartz and clay minerals rich in carbonaceous matter. The chert of the upper unit is also carbonaceous and rich in radiolarian remains. The lower and middle units are correlated with the *Neoalbaillella optima* Zone (Changhsingian). The basal part of the upper unit is referable to the *Hindeodus parvus* Zone (basal Griesbachian), and the major part of the upper unit is possibly correlated with the middle to upper Dienerian. We position the PTB at the sharp lithologic boundary between the upper Upper Permian chert and lower Lower Triassic black claystone.
The examined PTB siliceous rocks are stratigraphically attributed to the upper part of the Hashikadani Formation, reconstructed as an oceanic rock unit characterized by Lower Permian to Lower Triassic siliceous rocks that accumulated upon the lower flank of a mid-oceanic seamount in a pelagic realm of the Panthalassa Ocean. Our results present the world's first record of deep-marine PTB siliceous rocks associated with a Panthalassan seamount.

Key words: ***Hindeodus parvus*, Mino terrane, *Neoalbaillella optima* Zone, Panthalassa Ocean, Permian-Triassic Boundary, siliceous rocks**

Introduction

The approximately 251 Ma Permian-Triassic boundary (PTB) is known as an interval of the most profound collapse of marine and terrestrial ecosystems and drastic environmental devastation in the Phanerozoic (Erwin, 2006). Approximately 90% of marine and terrestrial species rapidly became extinct at the end of the Permian, resulting in the Phanerozoic's largest biotic turnover (Sepkoski, 1984; Bowring *et al.*, 1998). Concurrently, many shallow shelf seas suffered from euxinic to anoxic and sulfidic conditions during the Permian-Triassic transition (e.g., Wignall and Hallam, 1992; Nielsen and Shen, 2004; Wignall *et al.*, 2005; Cao *et al.*, 2009; Grasby and Beauchmap, 2009; Bond and Wignall, 2010).

The PTB biotic turnover and environmental changes have been mostly studied in shallow-marine carbonate and siliciclastic successions of the Tethyan platforms and peri-Pangean shelves (e.g., Payne *et al.*, 2004; Pruss *et al.*, 2006; Knoll *et al.*, 2007; Lehrmann *et al.*, 2007; Lindström and McLaughlin, 2007; Bond and Wignall, 2010; Korte and Kozur, 2010). The great deal of work in these regions has greatly contributed to the increase in our knowledge of the PTB crisis and its causes.

As suggested by Algeo *et al.* (2010), however, the PTB biotic and environmental crisis in the Panthalassa Ocean, estimated to be approximately 50% larger than the modern Pacific basin (Kiessling *et al.*, 1999), has been little studied to date. This is mainly due to the scarcity of reliable sections

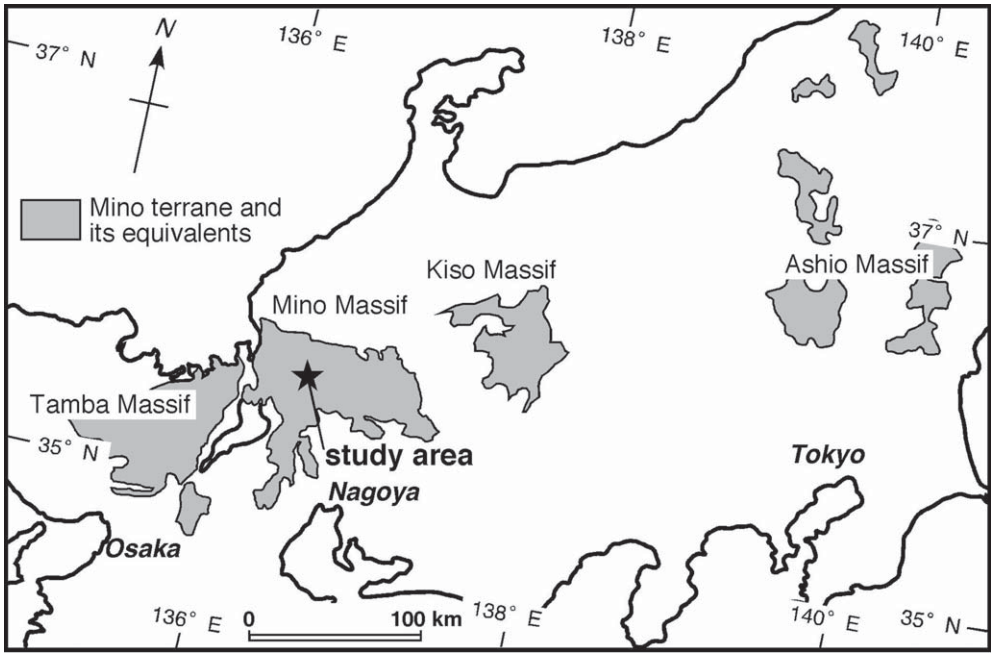

Figure 1. Locality of study area indicated by a star in the western part of Mino Massif, shown on the base map illustrating approximate distribution of the Mino terrane and its equivalents in central Japan, simplified after Nakae (2000).

from this region. Most of the Permian to Triassic Panthalassan ocean floor has been subducted and only a few seamounts (or oceanic plateaus) and deep-sea floors with sediments have survived as tectonic slivers and blocks within mélange units of accretionary terranes of the circum-Pacific region (North America: Monger *et al.* 1991; Orchard *et al.*, 2001; Japan: Isozaki, 1997a; Far East Russia and NE China: Kojima, 1989; New Zealand: Aita and Spörli 2007). Studies on the PTB crisis have been done in the face of the paucity of data from both shallow- and deep-marine sediments of the Panthalassa Ocean.

Since the discovery of the Permian-Triassic chert and black claystone of deep-marine, pelagic facies (Yamakita, 1987), several PTB siliceous-rocks sections have been reported from the Jurassic accretionary terranes of Japan (e.g., Ubara, Kyoto: Kuwahara *et al.*, 1991; Yamakita *et al.*, 1999; Gujo-hachiman, Gifu: Kuwahara *et al.*, 1998; Akkamori, Iwate: Takahashi *et al.*, 2009). Also, PTB siliceous rocks are reported from Arrow Rocks, New Zealand (Takemura *et al.*, 2002; Aita and Spörli 2007). The stratigraphic, paleontological, and geochemical studies of these siliceous rocks have provided significant data for the understanding of the PTB biotic turnover and environmental changes at great water depths in a pelagic realm of the Panthalassa Ocean (Kajiwara *et al.*, 1994; Takahashi *et al.*, 2009, 2010; Algeo *et al.*, 2010; Wignall *et al.*, 2010).

However, the basement rocks of these PTB siliceous rocks have mostly remained uncertain. Consequently, the sedimentary environment of the PTB siliceous rocks has been little understood.

In order to gain new insights into the depositional setting of the PTB siliceous rocks within the Panthalassa Ocean, we describe the lithostratigraphy and age of a stratigraphically intact section and two reference sections of the PTB siliceous rocks of the Mino terrane, for which the stratigraphic attribution is clear. The examined siliceous rocks correspond to the upper part of the Hashikadani Formation (Sano, 1988; emended by Kuwahara *et al.*, 2010), designated as a Lower Permian to Lower Triassic chert-dominant oceanic rock unit and reconstructed as having accumulated on the lower flank of a Panthalassan seamount. Our study area is in the Mt. Funabuseyama area, western Mino Massif, central Japan (Figure 1).

Geologic setting

Mino terrane

The Mino terrane is defined as a Jurassic subduction-generated accretionary complex of unmetamorphosed sedimentary rocks (Mizutani, 1990). The terrane rocks crop out in several separate areas of central Japan (Figure 1). The Mino Massif is one of the major exposure areas of the terrane rocks.

Major components of the Mino terrane comprise a terrigenous assemblage of sandstone and mudstone with a minor component of conglomerate referable to trench-fill deposits

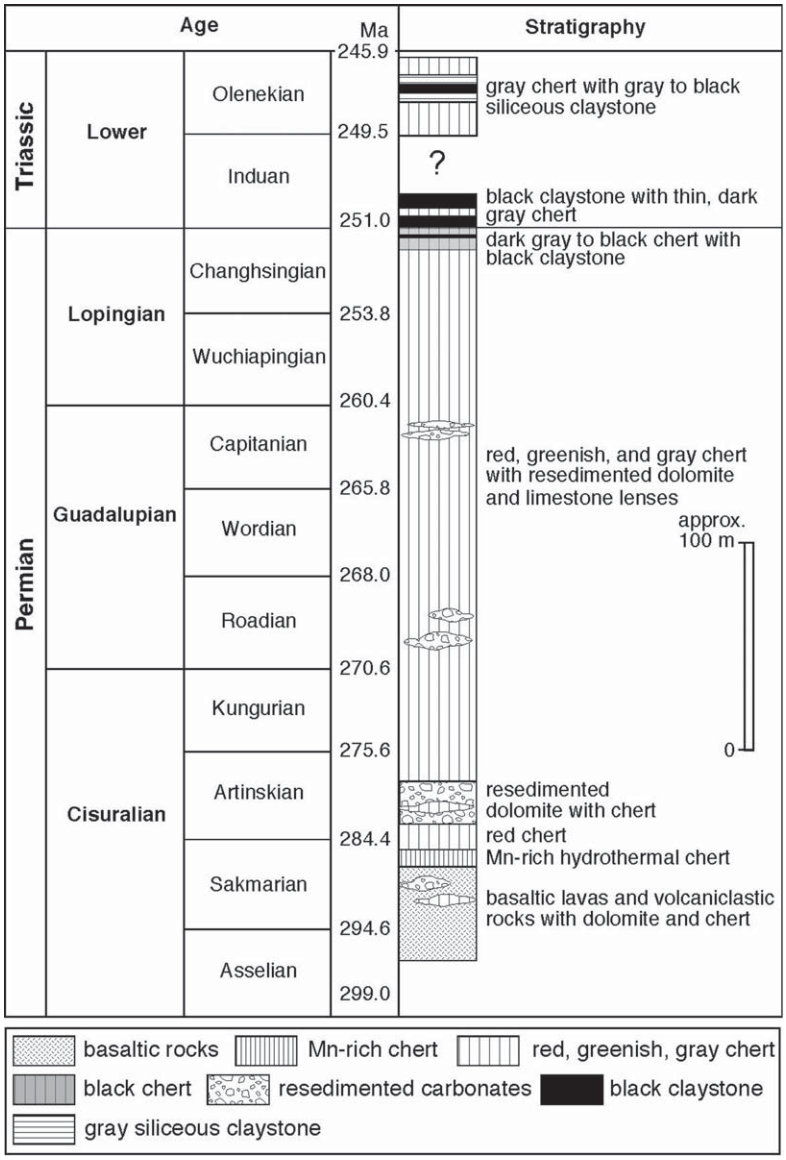

Figure 2. Revised stratigraphy of the Hashikadani Formation (Sano, 1988; emended by Kuwahara *et al.*, 2010).

(Takeuchi, 2000), and an oceanic assemblage of basaltic rocks, chert and related siliceous rocks, and carbonate rocks, formed in a mid-oceanic realm of the Panthalassa Ocean (Matsuda and Isozaki, 1991; Sano and Kojima, 2000). The former assemblage is mostly dated as Lower Jurassic to lowest Cretaceous, while the latter ranges from the Lower Permian to lowest Cretaceous (Wakita, 1988; Nakae, 2000). All these terrane rocks form a highly complicated imbricated structure of fault-bounded thrust sheets.

On the basis of the lithologic association, tectonostratigraphic properties, and age, Wakita (1988) divided the Mino terrane in Mino Massif into seven fault-bounded units, of which two are coherent units and five mélange units. Each of the coherent units is characterized by an orderly stratigraphic succession consisting of Lower Triassic siliceous claystone, Lower Triassic to upper Middle Jurassic chert, Lower Jurassic to lowest Cretaceous siliceous mudstone, and upper Middle Jurassic to lowest Cretaceous deep-water turbiditic sandstone and mudstone in ascending order. The succession represents a deep-water oceanic plate stratigraphy formed by lateral migration of depositional sites due to plate motion during Early Triassic to earliest Cretaceous time from a pelagic setting within a mid-oceanic realm to a trench area along a convergent margin (Matsuda and Isozaki, 1991). Mélange units are characterized by chaotic mixing of various-sized, disrupted, isolated slabs and blocks mainly of the Permian

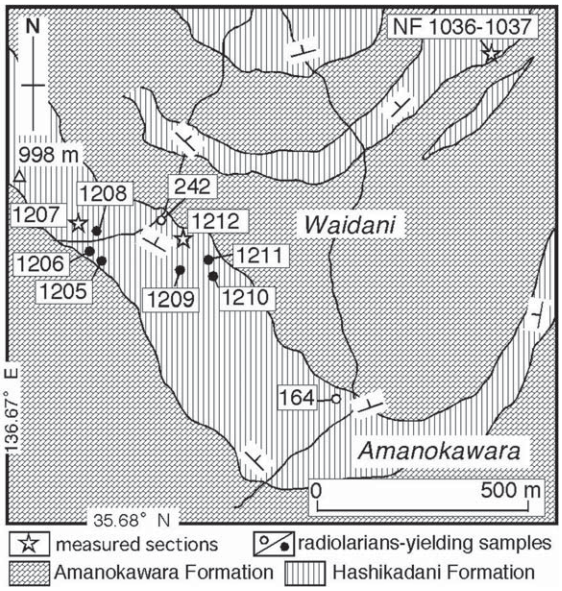

Figure 3. Simplified geologic map of the northwestern part of the Amanokawara plateau in the Mt. Funabuseyama area, western Mino Massif after Sano (1988). Localities of three measured sections of PTB siliceous rocks (locs. NF 1036–1037, 1207, and 1212) are indicated by stars. Open and solid circles show localities of Permian radiolarian fossils reported by Sano (1988) and extracted by the present study (Table 1), respectively.

to Jurassic oceanic assemblage with a matrix of Jurassic to lowest Cretaceous scaly mudstone. Dominant rock types of the slabs and blocks as well as the age of the mudstone matrix characterize each of the mélange units. For example, the Funabuseyama Unit, which includes the PTB siliceous rocks that we examined, is defined as a Middle Jurassic mélange unit characterized by large-sized slabs of Permian basaltic rocks, carbonates, and siliceous rocks with subordinate Triassic siliceous and carbonate rocks and a matrix of Middle Jurassic mudstone (Wakita, 1988).

Permian-Triassic oceanic assemblage in the Mt. Funabuseyama area

The Mt. Funabuseyama area is one of the major exposure areas of the Permian and associated Triassic oceanic rocks of the Mino terrane (Figure 1). Several fault-bounded slabs of the Permian-Triassic oceanic assemblage form the Funabuseyama mass, approximately 2 to 5 km wide and 15 km long or more, with narrow and laterally discrete, structurally interleaved wedges of Jurassic mudstone (Sano, 1988).

Sano (1988) divided the oceanic assemblage of the Mt. Funabuseyama area into three nearly time-equivalent stratigraphic units, namely, the Funabuseyama, Amanokawara, and Hashikadani formations. The former two are characterized by shallow-marine skeletal limestone and limestone breccia, respectively, both being underlain by basaltic rocks. The Hashikadani Formation is characterized by chert and related siliceous rocks underlain by basaltic rocks. Sano (1988) dated the Funabuseyama and Amanokawara formations as the late Early Permian to late Middle Permian and late Early Permian, respectively. The Hashikadani Formation ranges from the middle Lower Permian to upper Lower Triassic (Figure 2: Sano, 1988; emended by Kuwahara *et al.*, 2010). Sano (1988) and Sano *et al.* (1992) interpreted the Funabuseyama, Amanokawara, and Hashikadani formations as sediments at the top, on the upper flank, and on the lower flank of a mid-oceanic seamount, respectively. The geochemical property of the basaltic rocks of these three units (Jones *et al.*, 1993) supports the interpretation by Sano (1988) and Sano *et al.* (1992).

Hashikadani Formation

The Hashikadani Formation begins with a basal basaltic unit directly overlain by hydrothermally precipitated Mn-rich chert, which is, in turn, followed by a middle Lower Permian to uppermost Permian radiolarian chert succession (Figure 2). The chert succession contains resedimented carbonates chiefly of dolomite breccia with subordinate dolomite sandstone, displaced down from a shallow-marine carbonate buildup of the Amanokawara Formation on the upper flank of the seamount. The uppermost part of the Hashikadani Formation consists of gray, dark gray, and black cherts, gray to greenish gray siliceous claystone, and highly carbonaceous black claystone, and caps the age of the formation as late Early Triassic (Kuwahara *et al.*, 2010). The examined PTB siliceous rocks stratigraphically correspond to the upper part of the Hashikadani Formation (Figure 2).

The examined PTB siliceous rocks crop out in the northwestern part of the Amanokawara plateau to the north of Mt. Funabuseyama, where the carbonate and basaltic rocks of the Amanokawara Formation and siliceous rocks of the Hashikadani Formation dominantly crop out (Figure 3; Sano, 1988). The two oceanic-rock units are in fault contact with each other, and form a gentle synform, the fold axis of which is inclined to the north.

We measured three sections of the PTB siliceous rocks at localities NF 1036–1037, 1207, and 1212 (Figure 3). The three sections are included in two slabs composed dominantly of Middle to Upper Permian chert with minor Lower Triassic siliceous rocks of the Hashikadani Formation. One of the two sheets yields Middle to late Late Permian radiolarians at several localities (NF 164 and NF 242: Sano, 1988; NF 1205 to NF 1211: Figure 3; Table 1).

Lithostratigraphy of PTB siliceous rocks

Our examination revealed that the NF 1212R section measured at loc. NF 1212 comprises a stratigraphically fully con-

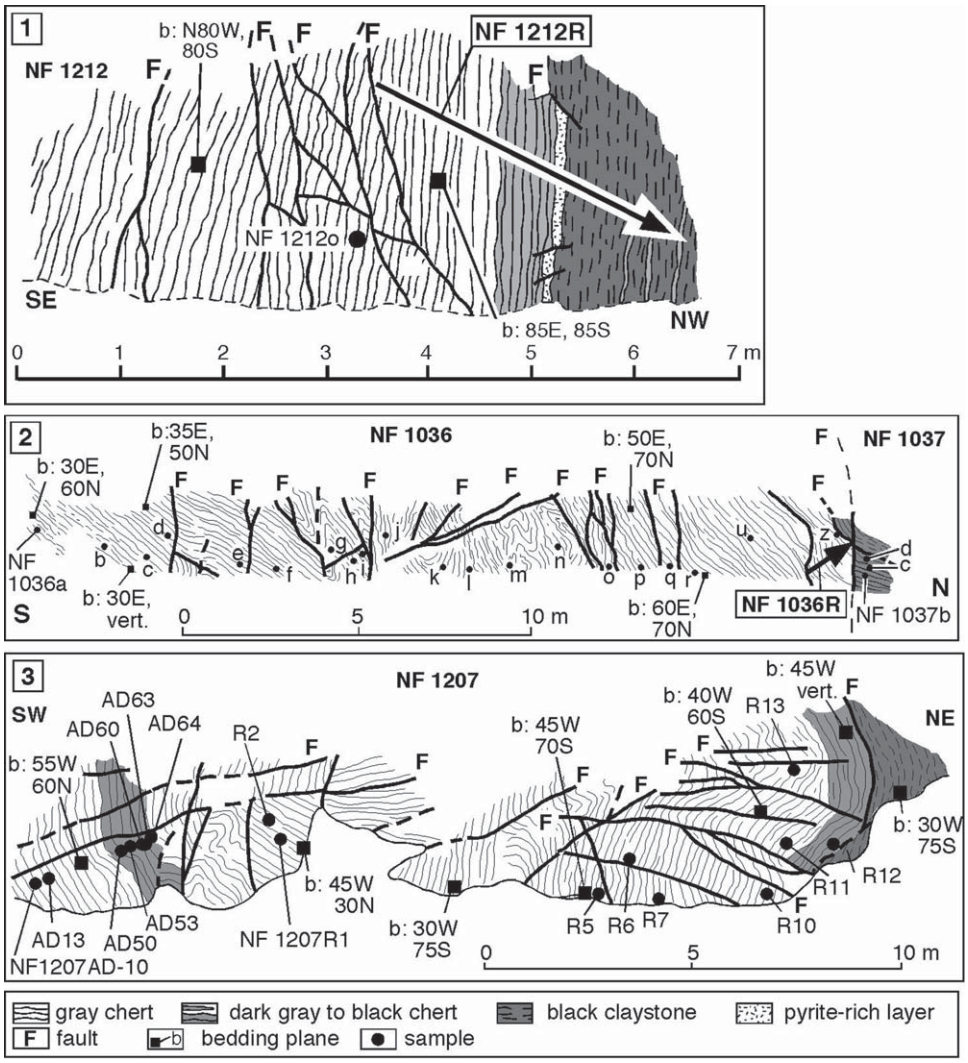

Figure 4. Field sketches illustrating the relationship between dark gray to black chert and black claystone of the Hashikadani Formation on the Amanokawara plateau. Solid circles indicate sites of radiolarian-yielding samples listed in Table 1. See Figure 3 for localities. F: fault. **1.** Stratigraphically intact succession of the Upper Permian chert and Lower Triassic black claystone of the NF 1212R section. Loc. NF 1212. **2.** Fault contact between intensely faulted and folded middle Middle to upper Upper Permian chert and presumably Lower Triassic black claystone. Locs. NF 1036–1037. The topmost part of the Upper Permian chert was measured as NF 1036R in Figure 5-2. **3.** Fault contact between complexly contorted upper Middle Permian to upper Upper Permian chert and presumably Lower Triassic black claystone. Loc. NF 1207.

tinuous succession of uppermost Permian chert and lower Lower Triassic black claystone. The radiolarian and conodont biostratigraphic examinations accurately positioned the stratigraphic level of the PTB in the NF 1212R section. We regard it as the best of the PTB siliceous rocks sections of the Hashikadani Formation in the Mt. Funabuseyama area. Also, we measured the PTB siliceous rocks at localities NF 1036–1037 and 1212 as reference sections.

NF 1212R section

Most of the beds of the NF 1212R section are nearly vertical and occasionally steeply dipping to the south, but face north-northwest (Figure 4-1). The NF 1212R section comprises a lower unit of gray bedded chert (ca. 1.7 m thick), a middle unit of dark gray to black chert (ca. 0.8 m) followed by a chocolate brown-weathered, presumably pyrite-rich layer (ca. 0.1 m), and an upper unit of black claystone with thin, dark gray to black chert beds (ca. 1.2 m) in ascending order (Figure 5-1). The three units are conformable with each other without marked stratigraphic disruption (Figure 6-1, 3). The bottom of the section is in fault contact with the gray chert that yields *Neoalbaillella ornithoformis,* indicative of the middle Late Permian (NF 1212o in Figure 4-1; Figure 9-5; Table 1), and talus deposits cover the top of

Table 1. A list of middle Middle to late Late Permian radiolarians extracted from chert of the Hashikadani Formation in Amanokawara plateau. Localities of samples of NF 1037, 1036, and 1036R, samples NF 1205, 1206, 1208, 1209, and 1211, samples of NF 1207R and 1207AD, and sample NF 1212o are indicated in Figure 4-2, Figure 3, Figure 4-3, and Figure 4-1, respectively. Stratigraphic levels of the samples of NF 1036R section are shown in Figures 5-2.

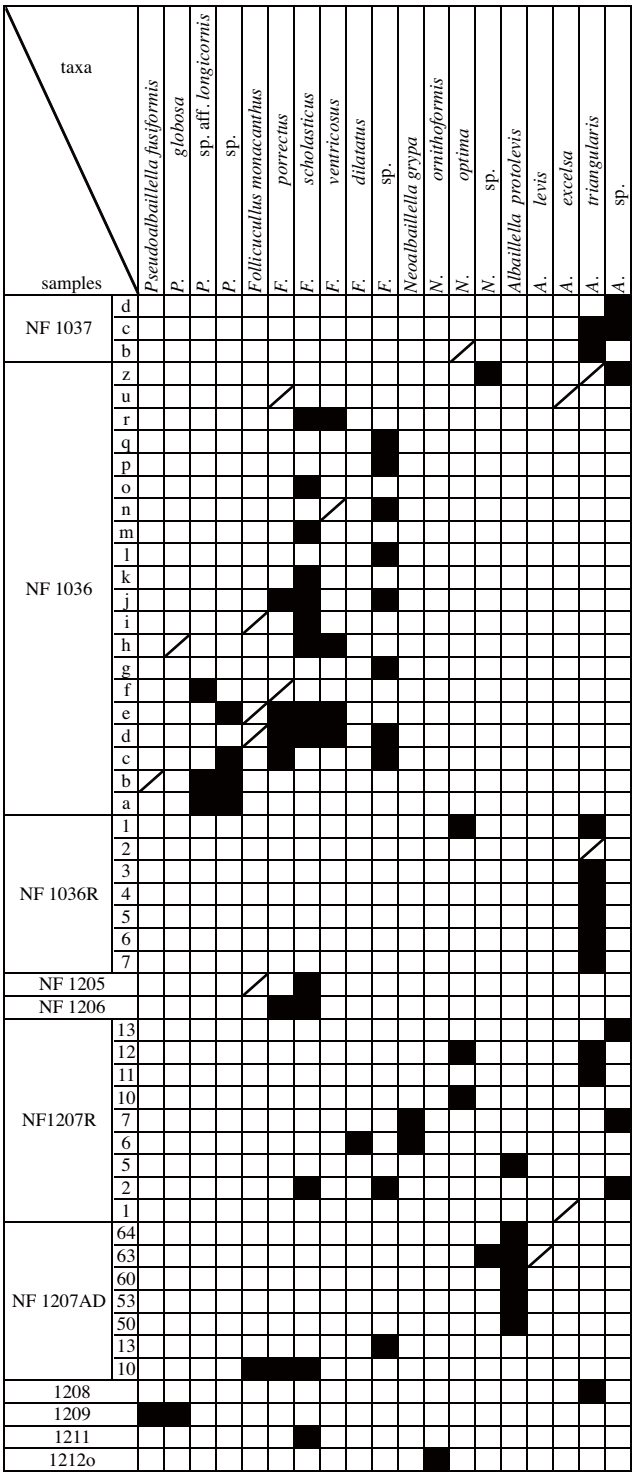

the upper unit. Throughout the NF 1212R section, neither coarse-grained terrigenous nor volcanic materials are recognized both in the field and under the microscope.

The lower unit dominantly comprises gray chert with minor greenish gray chert. Each bed is mostly 2 to 5 cm thick and alternates with gray to greenish gray clayey partings, usually less than 1 cm thick (Figure 6-2).

The middle unit consists of dark gray to black chert alternating with black claystone partings (Figure 6-2) with a chocolate brown-weathered silty layer at the top (Figure 6-3). The thickness of the black claystone partings of the middle unit tends to slightly increase up-section (Figure 5-1).

Under the microscope, the dark gray to black chert of the middle unit dominantly comprises radiolarian remains and subordinately rod-shaped sponge spicules with tapering ends (Figure 7-1). These siliceous organic debris are set in a matrix of microcrystalline quartz with a great admixture of fine-grained carbonaceous matter. Tiny pyrite grains are scattered both in the siliceous organic debris and matrix.

A chocolate brown-weathered silty layer, approximately 10 cm thick, overlies the black chert at the top of the middle unit (Figure 6-3). Both its lower and upper boundaries are clearly defined. It includes faint vestiges of parallel laminae. Though its primary lithologic properties have been completely lost due to deep weathering, we infer it to have been a pyrite-rich bed on the basis of a comparison of its stratigraphic position with conspicuous, fist-sized pyrite nodules at the top of the upper Upper Permian chert unit immediately below the lowest Triassic black claystone of another PTB siliceous-rocks section (Sano *et al.*, 2010).

The upper unit comprises a black claystone and contains thin beds of black to dark gray chert at a few levels (Figure 5-1). The black claystone is highly fissile (Figure 6-4), extremely fine-grained, and highly carbonaceous. Gray parallel laminae are occasionally faintly discerned in the black claystone. The intercalated chert beds are 1 to 5 cm thick, and have well defined top and bottom surfaces.

The black claystone of the upper unit comprises a mixture of clay minerals and cryptocrystalline quartz with a great admixture of extremely fine carbonaceous matter and contains a small amount of flattened radiolarian remains (Figure 7-3, 4). The gray parallel laminae are less carbonaceous, with poorly defined top and bottom surfaces (Figure 7-4). The chert intercalated in the upper unit essentially consists of radiolarian remains and contains scattered, tiny pyrite grains (Figure 7-2).

NF 1036R section

Chert and black claystone lithologically comparable with those of section NF 1212R crop out at loc. NF 1036–1037 (Figure 3). Though the chert and black claystone are in fault contact with each other, we measured the chert immediately below the black claystone at loc. NF 1036–1037 as reference

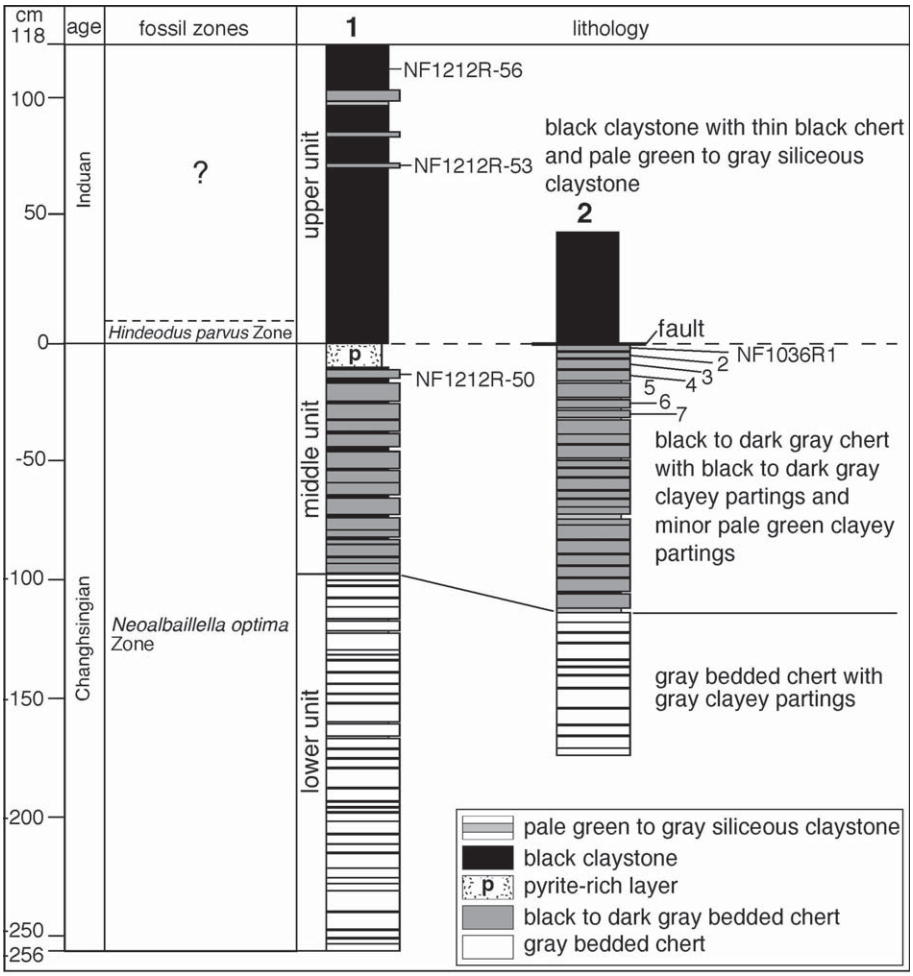

Figure 5. Stratigraphic columnar sections of the PTB siliceous rocks of the Hashikadani Formation. See Figure 3 for locality. **1.** Completely intact PTB siliceous rock succession. NF 1212R. **2.** Faulted PTB siliceous rock succession. NF 1036R.

section NF 1036R (Figure 4-2). On the basis of radiolarian biostratigraphic examination, the chert at loc. NF 1036–1037 is younging to the north over the whole of the exposure, ranging from the middle Middle Permian in the lower part to the upper Upper Permian in the upper part (Table 1).

The NF 1036R section attains approximately 1.7 m in thickness and entirely comprises a bedded chert unit, consisting of gray chert in the lower part and dark gray to black, carbonaceous chert in the upper part (Figure 5-2). Tiny pyrite grains are often discerned in the black chert. These lithologic characteristics are closely similar to those of the middle unit of section NF 1212R (Figure 5).

Though separated from the underlying black to dark gray chert by faults, the black claystone above section NF 1036R is lithologically closely comparable with the black claystone in the upper unit of section NF 1212R (Figure 5). The rocks are sooty black to dark gray, very fine-grained, carbonaceous, and highly fissile.

NF 1207 section

Chert and black claystone lithologically comparable to those of locs. NF 1212 and NF 1036–1037 crop out at loc. NF 1207, approximately 300 m west-northwest of loc. NF 1212 within the same chert slab (Figure 3). The rocks at loc. NF 1207 have been, however, more intensely sheared by faults than those at loc. NF 1212 and in places overturned by complex folds (Figure 4-3). The boundary between the dark gray to black chert and black claystone has been faulted. Nevertheless, radiolarian biostratigraphic examination indicates that the chert of the NF 1207 section is younging to the northeast over the whole of the exposure and is structurally repeated at least twice (Figure 4-3; Table 1).

Chert of the NF 1207 section is usually gray, dark gray, and black, occasionally reddish and greenish gray. The chert immediately below the black claystone and yielding the latest Permian radiolarians is black to dark gray (Figure 4-3; Table 1). The black claystone at the top of section NF 1207 is ex-

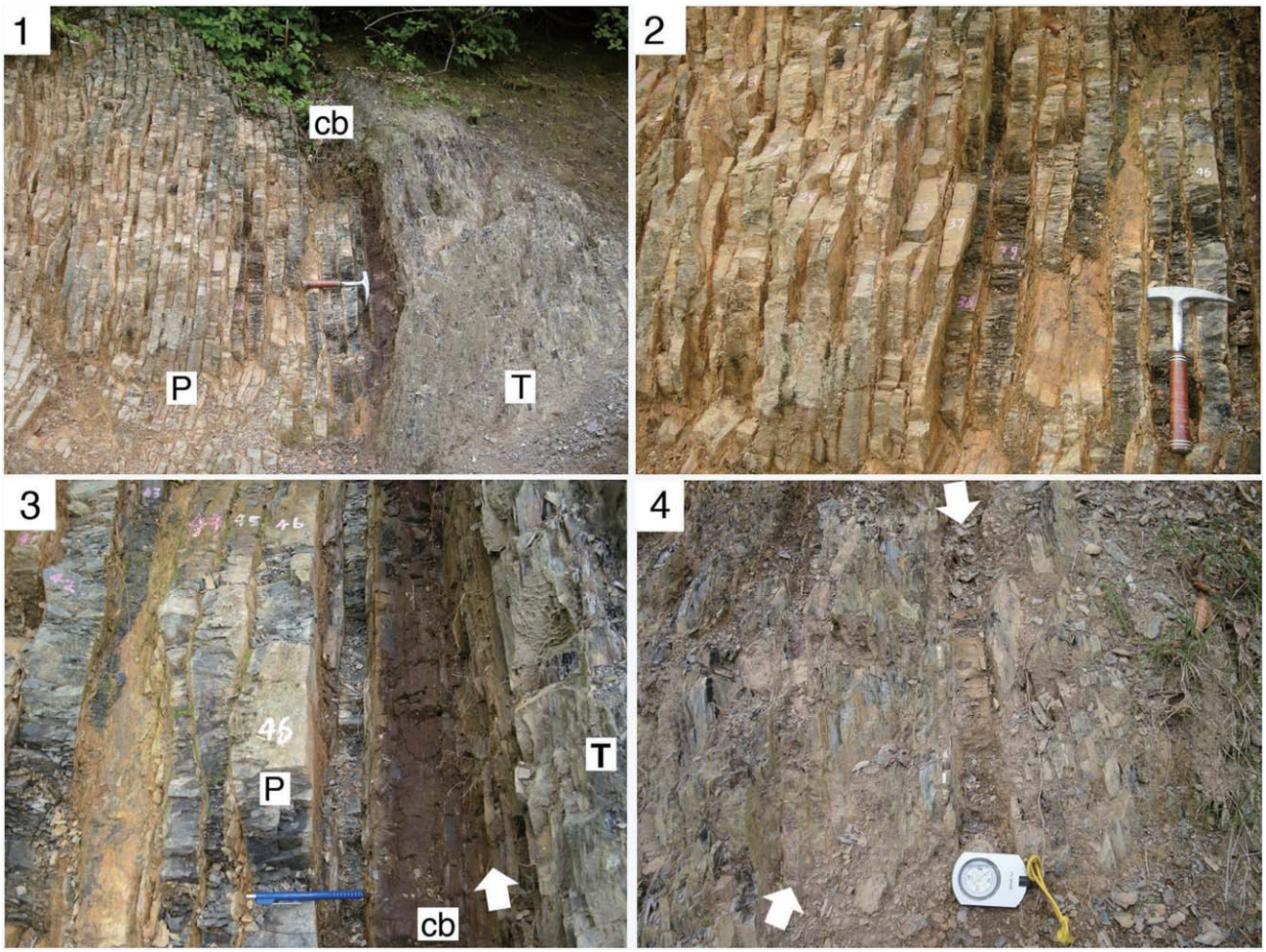

Figure 6. Outcrop views of the PTB siliceous rocks of the NF 1212R section. See Figures 3 and 4-1 for locality and field sketch, respectively. **1.** Entire view of section NF 1212R showing the nearly vertically dipping upper Upper Permian chert (P), chocolate brown-weathered, presumably pyrite-rich layer (cb), and Lower Triassic black claystone (T). The Permian-Triassic boundary is positioned at the base of the black claystone. **2.** Close-up view of the upper Upper Permian black to dark gray chert (right of view) and underlying gray chert (left). **3.** Close-up view of the sharp lithologic boundary between the upper Upper Permian black to dark gray chert (P), chocolate brown layer (cb), and lowest Triassic black claystone (T). An arrow indicates the most likely stratigraphic position of the Permian-Triassic boundary. **4.** Lower Triassic black claystone with thin intercalated beds of black to dark gray chert, indicated by arrows.

tremely fine-grained and carbonaceous. The black to dark gray chert and black claystone at the top of section NF 1207 are lithologically comparable with the middle and upper units of section NF 1212, respectively. We consider that the chert and associated black claystone of section NF 1207 primarily comprise a PTB siliceous-rocks succession.

Biostratigraphy and age of PTB siliceous rocks

The PTB siliceous rocks were thoroughly dated by radiolarians and conodonts. The chert of the study area was examined by radiolarians and the black claystone of the upper unit of section NF 1212R section by conodonts.

Chert samples of sections NF 1212R and NF 1036R were collected bed by bed. We processed a total of 266 chert samples for the radiolarian biostratigraphic examination. The acid-processed residues were mounted in glass slides and observed using a biological microscope. In total, 906 photomicrographs were taken for the examination (798 for the lower and middle units and 108 for the upper unit).

Four samples of black claystone and intercalated black chert were examined for conodonts. The rock samples were crushed into thin chips for optical microscopic observations. Though most of the conodont elements have been dissolved, their molds remain well preserved enough for identification on the surfaces of the chips.

We follow Ishiga (1986), Kuwahara *et al.* (1998), and Xia *et al.* (2005) for the Permian radiolarian biostratigraphic

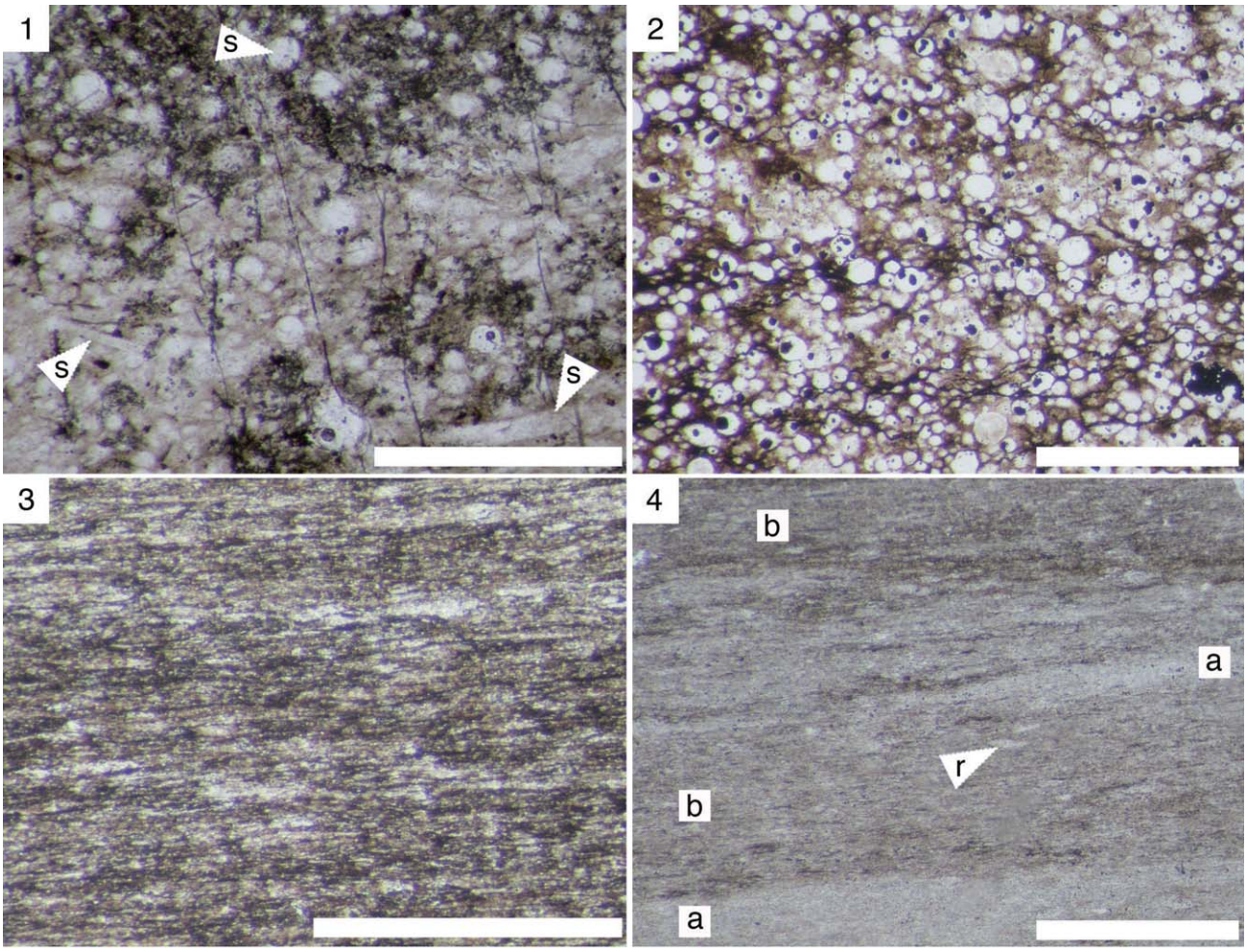

Figure 7. Thin-section photomicrographs of the upper Upper Permian chert and Lower Triassic chert and black claystone of section NF 1212R. Stratigraphic levels of samples are indicated in Figure 5-1. All scale bars=1 mm. Plane light. **1.** Radiolarian chert with minor siliceous sponge spicules (s) set in a matrix rich in extremely fine carbonaceous matter. Uppermost Permian. Top of the middle unit. NF 1212R-50. **2.** Carbonaceous black chert crowded with radiolarian remains. Tiny pyrite grains are widespread. Note higher concentration of carbonaceous matter along complexly anastomosing stylolite surfaces at bottom of view. Lower Triassic. Upper unit. NF 1212R-53. **3.** Black claystone composed of cryptocrystalline quartz and clay minerals with great admixture of fine carbonaceous matter. Lower Triassic. Upper unit. NF 1212R-56. **4.** Less carbonaceous, light-colored siliceous laminae (a), with poorly defined top and bottom surfaces in black claystone (b), with minor flattened radiolarian remains (r) discerned with poorly defined outlines. Lowest Triassic. Upper unit. NF 1212R-56.

zones and their age assignment. Triassic conodont biostratigraphic zones and their correlation are adopted from Jiang *et al.* (2007) and Zhao *et al.* (2007).

NF 1212R section

Permian radiolarian biostratigraphy.—We identified 56 species of 37 genera of radiolarians in the chert of the lower and middle units of the NF 1212R section (Figure 8). The preservation of the radiolarians is moderate, but tends to be poor up section. The radiolarians in the black to dark gray chert in the upper part of the middle unit are poorly preserved in comparison with those in the underlying beds.

Our examination revealed that the albaillellarian species characteristic of the *Neoalbaillella optima* Zone occur widely throughout the entire lower and middle units of section NF 1212R (Figure 8). The albaillellarian species include *Albaillella levis* (Figure 9-1), *A. triangularis* (Figure 9-2), *Albaillella*? sp. A (Figure 9-3), and *Neoalbaillella optima* (Figure 9-4). *A. levis,* which is diagnostic of the upper part of the middle Upper Permian *N. ornithoformis* Zone, is encountered only near the bottom of section NF 1212R (Figure 8). On the basis of the dominant occurrence of the radiolarians diagnostic of the *Neoalbaillella optima* Zone, we correlate the lower and middle units of section NF 1212R with the uppermost Permian (Changhsingian).

Along with these albaillellarian fossils, diverse species of

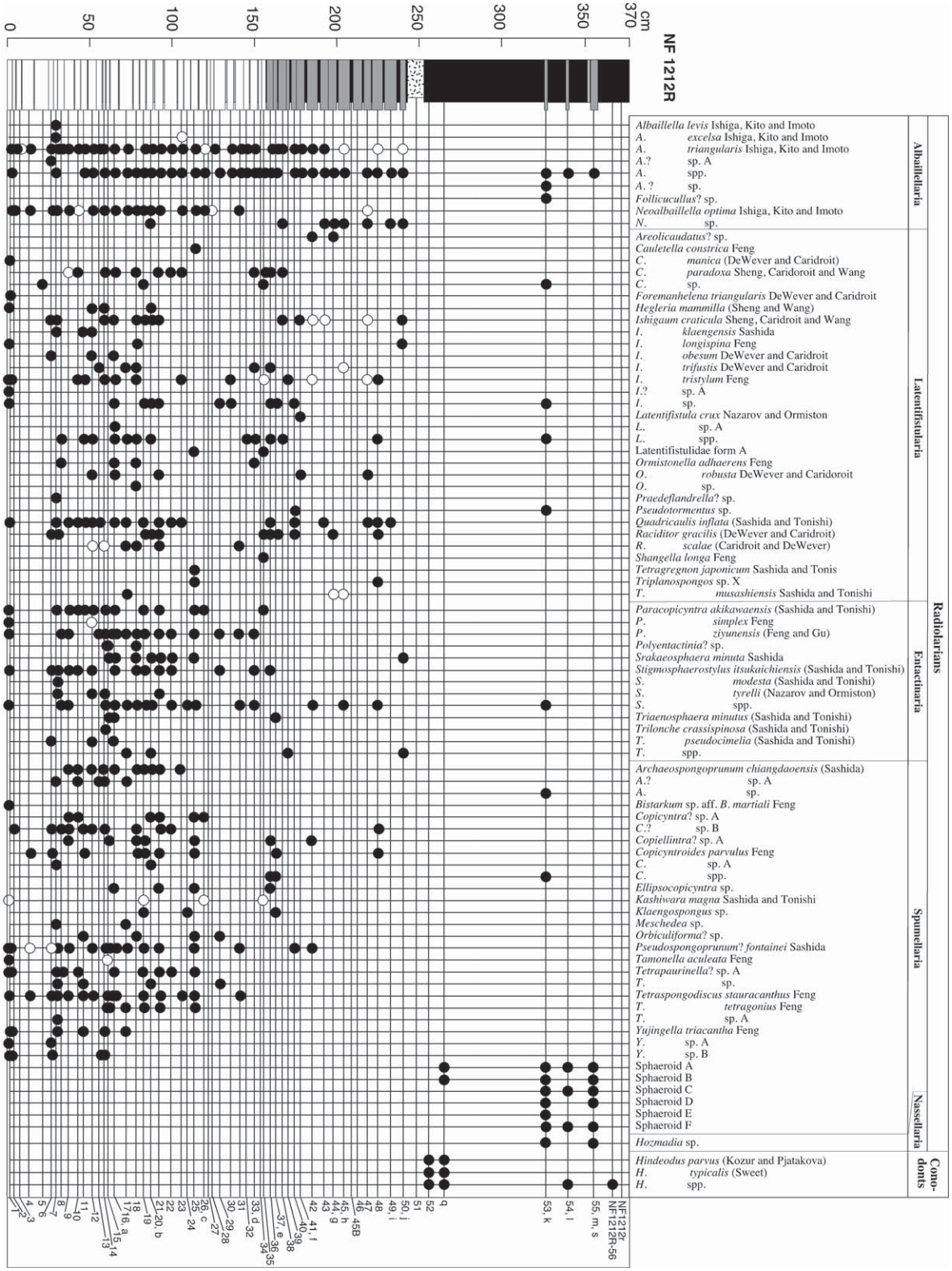

Figure 8. Stratigraphic distribution of Permian and Triassic radiolarians and Triassic conodonts in section NF 1212R. See Figure 5 for symbols for lithology in the columnar section. The classification of radiolarians into the four orders of Albaillellaria, Latentifistularia, Entactinaria, and Spumellaria chiefly follows De Wever *et al.* (2001) and Feng *et al.* (2006a, b).

the orders Latentifistularia, Entactinaria, and Spumellaria are extracted from the lower and middle units of section NF 1212R (Figure 8). Extracted are Latentifistularia including *Areolicaudatus*? sp. (Figure 9-6), *Cauletella constrica* (Figure 9-7), *C. manica* (Figure 9-8), *C. paradoxa* (Figure 9-9), *Foremanhelena triangula* (Figure 9-10), *Hegleria mammilla* (Figure 9-11), *Ishigaum craticula* (Figure 9-12), *I. klaengensis* (Figure 9-13), *I. longispina* (Figure 9-14), *I. obesum* (Figure 9-15), *I. trifustis* (Figure 9-16), *I. tristylum* (Figure 9-17), *I.*? sp. A (Figure 9-18), *Latentifistula crux* (Figure 9-19), *L.* sp. A (Figure 9-20), Latenfistulidae form A (Figure 9-21), *Ormistonella adhaerens* (Figure 9-22), *O. robusta* (Figure 9-23), *Quadricaulis inflata* (Figure 9-24), *Raciditor gracilis* (Figure 9-25), *R. scalae* (Figure 9-26), *Shengella longa* (Figure 9-27), *Tetragregnon japonicum* (Figure 9-28), *Triplanospongos musashiensis* (Figure 9-29), Entactinaria including *Copicyntra*? sp. A (Figure 9-30), *Copicyntra*? sp. B (Figure 10-1), *Paracopicyntra akikawaensis* (Figure 10-2), *P. simplex* (Figure 10-3), *P. ziyunensis* (Figure 10-4), *Polyentactinia*? sp. (Figure 10-5), *Srakaeosphaera minuta* (Figure 10-6), *Stigmosphaerostylus itsukaichiensis* (Figure 10-7), *S. modesta* (Figure 10-8), *S. tyrelli* (Figure 10-9), *Triaenosphaera minutus* (Figure 10-10), *Trilonche crassispinosa* (Figure 10-11), and *T. pseudocimelia* (Figure 10-12), and Spumellaria including *Archaeospongoprunum chiangdaoensis* (Figure 10-13), *A.*? sp. A (Figure 10-14), *Bistrakum* sp. aff. *B. martiali* (Figure 10-15), *Copiellintra*? sp. A (Figure 10-16), *Copicyntroides parvulus* (Figure 10-17), *Copicyntroides*? sp. A (Figure 10-18), *Kashiwara magna* (Figure 10-19), *Meschedea* sp. (Figure 10-20), *Orbiculiforma*? sp. (Figure 10-21), *Pseudospongoprunum*? *fontainei* (Figure 10-22), *Tamonella aculeanta* (Figure 10-23), *Tetrapaurinella*? sp. A (Figure 10-24), *Tetraspongodiscus stauracanthus* (Figure 10-25), *Tetraspongodiscus tetragonius* (Figure 10-26), *T.* sp. A (Figure 10-27), *Yujingella triacantha* (Figure 10-28), *Y.* sp. A (Figure 10-29), and *Y.* sp. B (Figure 10-30). Characteristically, radiolarian species having spongy tests (e.g., *Paracopicyntra ziyunensis* of Figure 10-4; *Pseudospongoprunum*? *fontainei* of Figure 10-22) are dominantly yielded in the lower and middle units of section NF 1212R.

Triassic radiolarian biostratigraphy.—Our examination revealed that *Hozmadia* sp. (Figure 11-1 to 4) occurs in the chert beds at three levels in the upper part of the upper unit of section NF 1212R (Figure 8). The radiolarian assemblage of the upper two levels is of low diversity and characterized by an almost exclusive dominance of sphaeroid forms (Figure 11-6, 8 to 13).

Hozmadia was originally designated as a new genus (type species: *Hozmadia reticulata*) of Nassellaria by Dumitrica *et al.* (1980) from the Anisian-Ladinian boundary horizon of the Southern Alps. Sugiyama (1992) defined the *Hozmadia gifuensis* Assemblage characterized by many characteristic species of Nassellaria and Spumellaria in a chert section of the Mino terrane, central Japan. Sugiyama (1992) considered the *H. gifuensis* Assemblage as indicating the early Anisian. Kamata *et al.* (2007) reported the occurrence of *Hozmadia* with Triassic-type nassellarians, including *Tripedocorbis, Tripedocassis*, and *Triassospongocyrtis*, from a chert sequence at Arrow Rock, New Zealand, correlated with the upper Dienerian *Neospathodus dieneri* and *N. cristagalli* zones. On the basis of the reported stratigraphic range of *Hozmadia*, the upper half of the upper unit of section NF1212R is possibly assignable to the upper Dienerian.

The black claystone immediately above the base of the upper unit of section NF1212R (NF 1212q in Figure 8) yields only sphaeroid radiolarians (Figure 11-5 and 7). However, these radiolarians are not useful for age determination.

The careful examination revealed the enigmatic fact that some Permian-type radiolarians occur in the chert beds within the Induan black claystone of the upper unit of section NF 1212R (Figure 8). The enigmatic radiolarians include *Albaillella* spp. (Figure 11-23 to 26), *Follicucullus*? sp. (Figure 11-29), *Cauletella* sp. (Figure 11-19), *Latentifistula* sp., *Stigmosphaerostylus* sp. (Figure 11-16 to 18), and *Copicyntroides* sp. (Figure 11-15). Except for *Follicucullus*? sp., these radiolarians are yielded also in the lower and middle units.

Triassic conodont biostratigraphy.—We identified two species of one genus of conodonts from the black claystone of the upper unit of section NF 1212R. Age-reliable conodonts include P1 elements of *Hindeodus parvus* (Kozur and Pjatakova) and *H. typicalis* (Sweet), yielded from two very closely spaced levels within an approximately 15-cm-thick stratigraphic interval immediately above the base of the black claystone (NF 1212q and NF 1212R-52 in Figure 8). Also, Agematsu *et al.* (2010) found natural assemblages of *H. parvus* and *H. typicalis* in the black claystone at these two levels.

Hindeodus parvus (Figure 12-1 to 3) is the characteristic species of the *H. parvus* Zone, indicative of the basal Griesbachian (Yin *et al.*, 2001; Jiang *et al.*, 2007). Also, it is widely accepted that *H. parvus* is an index fossil for the Permo-Triassic boundary (Meishan: Lai *et al.*, 2001; Jiang *et al.*, 2007; Abadeh: Korte *et al.*, 2004; Spiti: Orchard and Krystyn, 1998).

H. typicalis (Figure 12-4, 5) is known to have a longer biostratigraphic range than *H. parvus* and occurs on both sides of the PTB transition (Sweet *et al.*, 1971; Zhao *et al.*, 2007). Jiang *et al.* (2007) reported, for example, the occurrence of *H. typicalis* from the *H. latidentatus* Zone (bed 24a of Meishan section A) to *Isarcicella staeschei* Zone (bed 29a), correlated with the Changhsingian and lower Induan, respectively. On the basis of the cooccurrence of *H. parvus* and *H. typicalis*, we correlate the basal 15-cm-thick stratigraphic interval of the upper unit of section NF 1212R with the lowest Triassic (basal Griesbachian) *H. parvus* Zone (Fig-

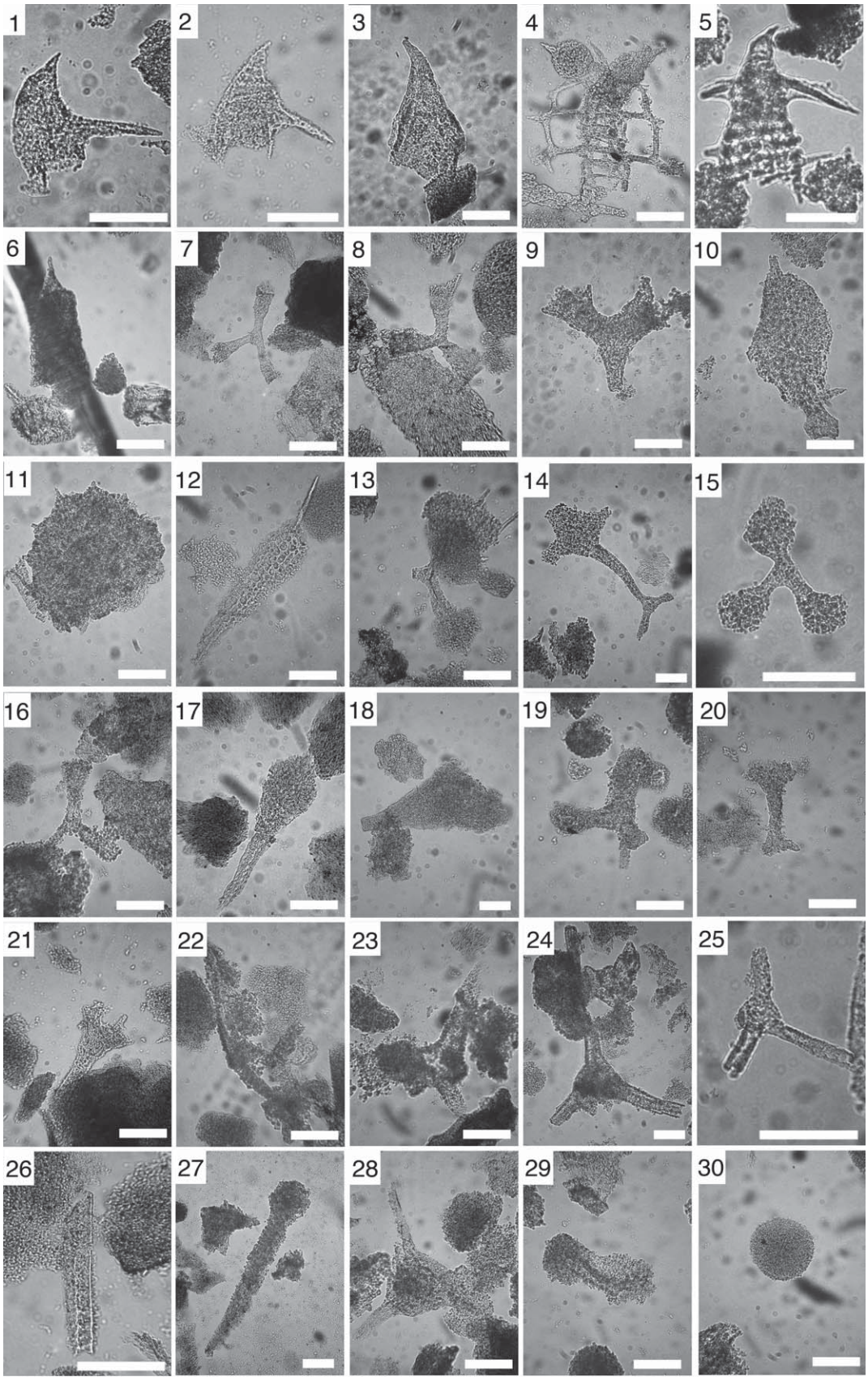
1
2
3
4
5
6
7
8
9
10
11
12
13
14
15
16
17
18
19
20
21
22
23
24
25
26
27
28
29
30

ure 8).

No reliable conodonts for precise age determination are yielded by the black claystone above the *H. parvus* Zone of section NF 1212R. Only a few species of *Hindeodu*s are recognized at two levels in the upper part of the upper unit (Figure 8). *Hindeodus* is reported to occur from the lower Lower Triassic sections of many areas (e.g., Kozur, 1988: Orchard and Krystyn, 1998). Its last occurrence is thought to date to the mid-Induan (latest Griesbachian or earliest Dienerian: Orchard, 2007). Based on the stratigraphic range of *Hindeodus*, the major part of the upper unit above the *H. parvus* Zone is broadly correlated with the middle Induan.

Age assignment of the entire NF 1212R section.—As described above, the chert of the lower and middle units of section NF 1212R is no doubt correlated with the upper Upper Permian (Changhsingian: Figure 5). The occurrence of conodonts characteristic of the *Hindeodus parvus* Zone indicates the basal part of the upper unit is correlated with the lowest Triassic (basal Griesbachian: Figure 5). On the basis of the combined age constraint by radiolarians and conodonts, the major part of the upper unit above the *H. parvus* Zone of section NF 1212R is correlated broadly with the Induan (Figure 5), possibly with the middle to upper Dienerian.

NF 1036R section

Comparably with section NF 1212R, the uppermost part of section NF 1036R also yields *A. triangularis,* which is characteristic of the *N. optima* Zone at several levels (Table 1). Though no reliable radiolarians were detected from the remaining part of section NF 1036R, we refer its entire succession to the *N. optima* Zone and correlate it with the middle unit of section NF 1212R (Figure 5).

NF 1207 section

Bedded chert of the basal part of loc. NF 1207 yields some species of the genus *Follicucullus* characteristic of the upper Middle Permian *F. scholasticus* Zone (NF 1207AD-10 and 13 in Figure 4-3; Table 1). Above the basal chert is a dark gray chert yielding *A. protolevis* Kuwahara, diagnostic of the *Neoalbaillella ornithoformis* Zone (Kuwahara *et al.*, 1998: NF 1207AD-50, 53, 60, 63, and 64 in Figure 4-3). The chert of the remaining exposure yields radiolarians characteristic of the *F. scholasticus, N. ornithoformis*, and *N. optima* zones in ascending order (NF 1207R-1 to 13 in Table 1). The black to dark gray chert immediately below the black claystone is referable to the *N. optima* Zone. The distribution pattern of these radiolarian zones suggests that the upper Middle to uppermost Permian chert of section NF 1207 is structurally duplicated, though facing the northeast as a whole in the exposure.

Discussion

Stratigraphic position of Permian-Triassic boundary

On the basis of the first occurrence of *Hindeodus parvus*, indicative of the earliest Triassic (Yin *et al.*, 2001; Jiang *et al.*, 2007) from the basal part of the upper unit of section NF 1212R, we position the PTB at the stratigraphic level between NF 1212R-51 and 52 (Figure 8). This stratigraphic level corresponds to the clearly defined base of the black claystone of the upper unit of section NF 1212R (Figure 5).

Because of the absence of reliable fossils, the age of the pyrite-rich layer immediately below the black claystone of the upper unit remains uncertain (Figure 5). However, on the basis of the latest Permian age of the chert containing comparable pyrite nodules in another PTB siliceous-rocks section in the Mt. Funabuseyama area (Sano *et al.*, 2010), the pyritic layer of section NF 1212R is most likely uppermost Permian.

Permian-type radiolarians in the Lower Triassic: an enigma

Our examination revealed that the Late Permian-type Albaillellaria mostly disappear at the PTB, corresponding with the bottom of the upper unit of section NF 1212R (Figure 8). Also, most of the Latentifistularia, Entactinaria, and Spumellaria widespread throughout its lower and middle units disappear along with the Albaillellaria. The majority of the Late Permian-type radiolarians are thought to have become extinct at the end of the Permian (Figure 8). However, enigmatically some Permian-type radiolarians are detected from the chert

⬅ **Figure 9.** Late Permian radiolarians extracted from the chert of the lower and middle units of section NF 1212R section and the chert (NF 1212o) of loc. NF 1212. See Figure 8 for the stratigraphic levels of the samples from NF 1212R. The locality of sample NF 1212o is indicated in Figure 4-1. All scale bars=100 μm. **1.** *Albaillella levis* Ishiga, Kito and Imoto, NF1212R-7. **2.** *Albaillella triangularis* Ishiga, Kito and Imoto, NF1212R-12. **3.** *Albaillella*? sp. A, NF1212R-6. **4.** *Neoalbaillella optima* Ishiga, Kito and Imoto, NF1212R-12. **5.** *Neoalbaillella ornithoformis* Takemura and Nakaseko, NF1212o. **6.** *Areolicaudatus*? sp., NF1212R-42. **7.** *Cauletella constrica* Feng, NF1212R-25. **8.** *Cauletella manica* (DeWever and Caridroit), NF1212R-1. **9.** *Cauletella paradoxa* Sheng, Caridroit and Wang, NF1212R-23. **10.** *Foremanhelena triangula* DeWever and Caridroit, NF1212R-1. **11.** *Hegleria mammilla* (Sheng and Wang), NF1212R-1. **12.** *Ishigaum craticula* Sheng, Caridroit and Wang, NF1212R-7. **13.** *Ishigaum klaengensis* Sashida, NF1212R-12. **14.** *Ishigaum longispina* Feng, NF1212R-1. **15.** *Ishigaum obesum* DeWever and Caridroit, NF1212R-7. **16.** *Ishigaum trifustis* DeWever and Caridroit, NF1212R-13. **17.** *Ishigaum tristylum* Feng, NF1212R-2. **18.** *Ishigaum*? sp. A, NF1212R-1. **19.** *Latentifistula crux* Nazarov and Ormiston, NF1212R-41. **20.** *Latentifistula* sp. A, NF1212R-16. **21.** Latentifistulidae form A, NF1212R-25. **22.** *Ormistonella adhaerens* Feng, NF1212R-8. **23.** *Ormistonella robusta* DeWever and Caridroit, NF1212R-12. **24.** *Quadricaulis inflata* (Sashida and Tonishi), NF1212R-23. **25.** *Raciditor gracilis* (DeWever and Caridroit), NF1212R-6. **26.** *Raciditor scalae* (Caridroit and DeWever), NF1212R-12. **27.** *Shengella longa* Feng, NF1212R-35. **28.** *Tetragregnon japonicum* Sashida and Tonishi, NF1212R-25. **29.** *Triplanospongos musashiensis* Sashida and Tonishi, NF1212R-17. **30.** *Copicyntra*? sp. A, NF1212R-10.

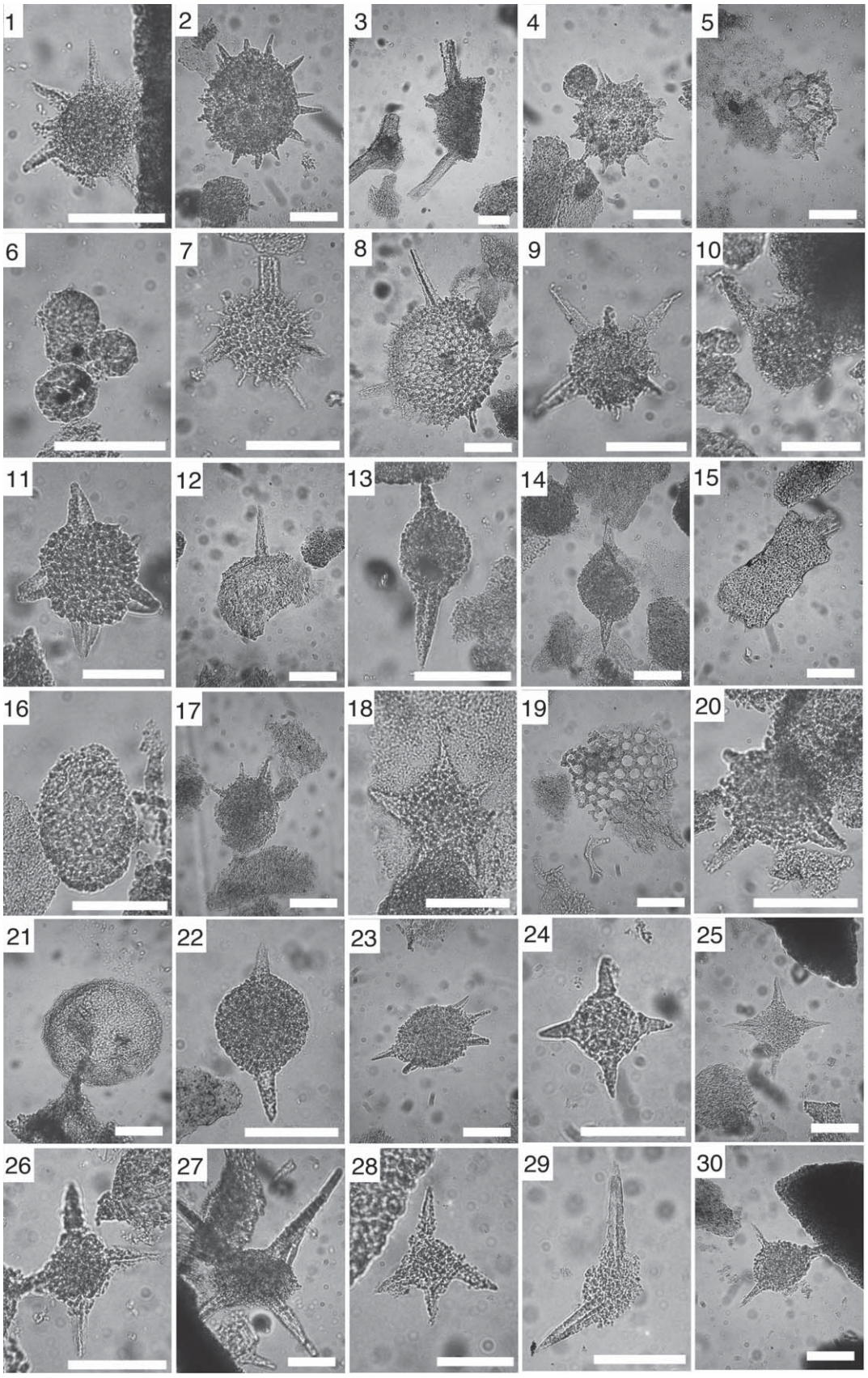
1
2
3
4
5
6
7
8
9
10
11
12
13
14
15
16
17
18
19
20
21
22
23
24
25
26
27
28
29
30

beds within the Induan black claystone of the upper unit of section NF 1212R.

Enigmatic occurrences of Permian-type radiolarians in the Lower Triassic have been documented in many areas (e.g., Mino Terrane: Sugiyama, 1992, 1997; Kuwahara *et al.*, 1991; Yao and Kuwahara, 1997; Far East Russia: Bragin, 1991; southern Thailand: Sashida *et al.*, 1998; South China: Feng *et al.*, 2000, 2001, 2007; Yao, 2009; Yao *et al.*, 2005; New Zealand: Takemura *et al.*, 2007). For example, Sugiyama (1997) reported the occurrence of *Follicucullus monacanthus*, *F. scholasticus*, *F. ventricosus*, *F*. sp., and *Latentifistula* sp. in the siliceous claystone and chert of the *Follicucullus–Parentactinia* Assemblage Zone, assigned to the early Spathian or older. Takemura *et al.* (2007) extracted many Permian-type radiolarian species from the Griesbachian to lower Dienerian chert sequence at Arrow Rocks, New Zealand.

To explain the enigmatic occurrence of Permian-type radiolarians, hypotheses emphasizing their survival across the PTB crisis and reappearance as Lazarus taxa (Kaufman and Erwin, 1995) in the Triassic seem to be favored by many radiolarian paleontologists (e.g., De Wever *et al.*, 2006; Feng *et al.*, 2007; Takemura *et al.*, 2007). For instance, Takemura *et al.* (2007) emphasized that Permian-type radiolarians survived across the PTB event into the Early Triassic. On the other hand, Yao (2009) regarded albaillellarians and latentifistularians from the upper Olenekian (Spathian) siliceous rocks as reworked species. Sugiyama (1992) recognized *Follicucullus*-bearing chert breccias embedded in Lower to Middle Triassic chert and demonstrated the reworking of Permian-type radiolarians into the Lower to Middle Triassic siliceous sediment.

It is conceivable that the enigmatic occurrence of Permian-type radiolarians in the Induan chert beds of section NF 1212R is due to their survival into Early Triassic time. Against this, the late Middle to early Late Permian genus *Follicucullus* likely occurs in the upper Upper Permian chert of NF 1212R, but is otherwise totally absent in this stratigraphic interval (Figure 8). Hence, it is possible that Permian-type radiolarians reappeared as Lazarus taxa in the Induan sediment of NF 1212, but, R. alternatively, it remains possible that some Permian-type radiolarians were reworked up into the Induan chert beds of NF 1212R. We need further sedimentological and paleontological studies to resolve this enigmatic occurrence of Permian-type radiolarians in the Induan sediment.

Depositional setting of PTB siliceous rocks

Though their age and biostratigraphy have been investigated in detail in several sections of PTB siliceous rocks, their stratigraphy in relation to the basement rocks has never been reconstructed, except for those at Arrow Rocks, New Zealand (Aita and Spörli, 2007). Even so, no attempt to infer the nature of the basement rocks and to make a stratigraphic attribution of PTB siliceous rocks has been made to date. It is chiefly because PTB siliceous rocks occur as small-sized, completely isolated blocks, which consist only of Upper Permian and Lower Triassic siliceous rocks, the underlying and overlying rocks having been tectonically detached. The shortage of knowledge on the basement rocks and stratigraphic attribution of the PTB siliceous rocks results in uncertainty concerning their depositional setting.

The measured PTB siliceous rocks crop out closely associated with the basaltic and dolomitic rocks and Middle Permian chert of the Hashikadani Formation (Figure 2: Sano, 1988; emended by Kuwahara *et al.*, 2010), all forming tectonic slabs on the Amanokawara plateau (Figure 3). Additionally the upper Upper Permian chert of the examined PTB siliceous rock sections is lithologically indistinguishable from the time-equivalent chert of the Hashikadani Formation near its type section. Thus, the examined PTB siliceous rocks are no doubt correlated with and attributed to the upper part of the Hashikadani Formation, reconstructed as a deep-marine chert-dominant facies that accumulated on the lower flank of a seamount in a pelagic realm (Sano, 1988; Sano *et al.*, 1992). We ascribe the examined PTB siliceous rocks to deep-marine sediments formed on the lower flank of a seamount in a pelagic realm of the Panthalassa Ocean. Our result presents the world's first documentation of deep-marine PTB siliceous rocks associated with a Panthalassan seamount.

⬅ **Figure 10.** Late Permian radiolarians extracted from the chert of the lower and middle units of NF 1212R section. See Figure 8 for the stratigraphic levels of the samples. All scale bars=100 μm. **1.** *Copicyntra*? sp. B, NF1212R-12. **2.** *Paracopicyntra akikawaensis* (Sashida and Tonishi), NF1212R-7. **3.** *Paracopicyntra simplex* Feng, NF1212R-1. **4.** *Paracopicyntra ziyunensis* (Feng and Gu), NF1212R-1. **5.** *Polyentactinia*? sp., NF1212R-14. **6.** *Srakaeosphaera minuta* Sashida, NF1212R-50. **7.** *Stigmosphaerostylus itsukaichiensis* (Sashida and Tonishi), NF1212R-7. **8.** *Stigmosphaerostylus modesta* (Sashida and Tonishi), NF1212R-7. **9.** *Stigmosphaerostylus tyrelli* (Nazarov and Ormiston), NF1212R-12. **10.** *Triaenosphaera minutus* Sashida and Tonishi, NF1212R-16. **11.** *Trilonche crassispinosa* (Sashida and Tonishi), NF1212R-7. **12.** *Trilonche pseudocimelia* (Sashida and Tonishi), NF1212R-6. **13.** *Archaeospongoprunum chiangdaoensis* (Sashida), NF1212R-12. **14.** *Archaeospongoprunum*? sp. A, NF1212R-7. **15.** *Bistarkum* sp. aff. *B. martiali* Feng, NF1212R-1. **16.** *Copiellintra*? sp. A, NF1212R-9. **17.** *Copicyntroides parvulus* Feng, NF1212R-11. **18.** *Copicyntroides*? sp. A, NF1212R-7. **19.** *Kashiwara magna* Sashida and Tonishi, NF1212R-1. **20.** *Meschedea* sp., NF1212R-17. **21.** *Orbiculiforma*? sp., NF1212R-29. **22.** *Pseudospongoprunum*? *fontainei* Sashida, NF1212R-2. **23.** *Tamonella aculeata* Feng, NF1212R-1. **24.** *Tetrapaurinella*? sp. A, NF1212R-7. **25.** *Tetraspongodiscus stauracanthus* Feng, NF1212R-7. **26.** *Tetraspongodiscus tetragonius* Feng, NF1212R-23. **27.** *Tetraspongodiscus* sp. A, NF1212R-7. **28.** *Yujingella triacantha* Feng, NF1212R-7. **29.** *Yujingella* sp. A, NF1212R-1. **30.** *Yujingella* sp. B, NF1212R-2.

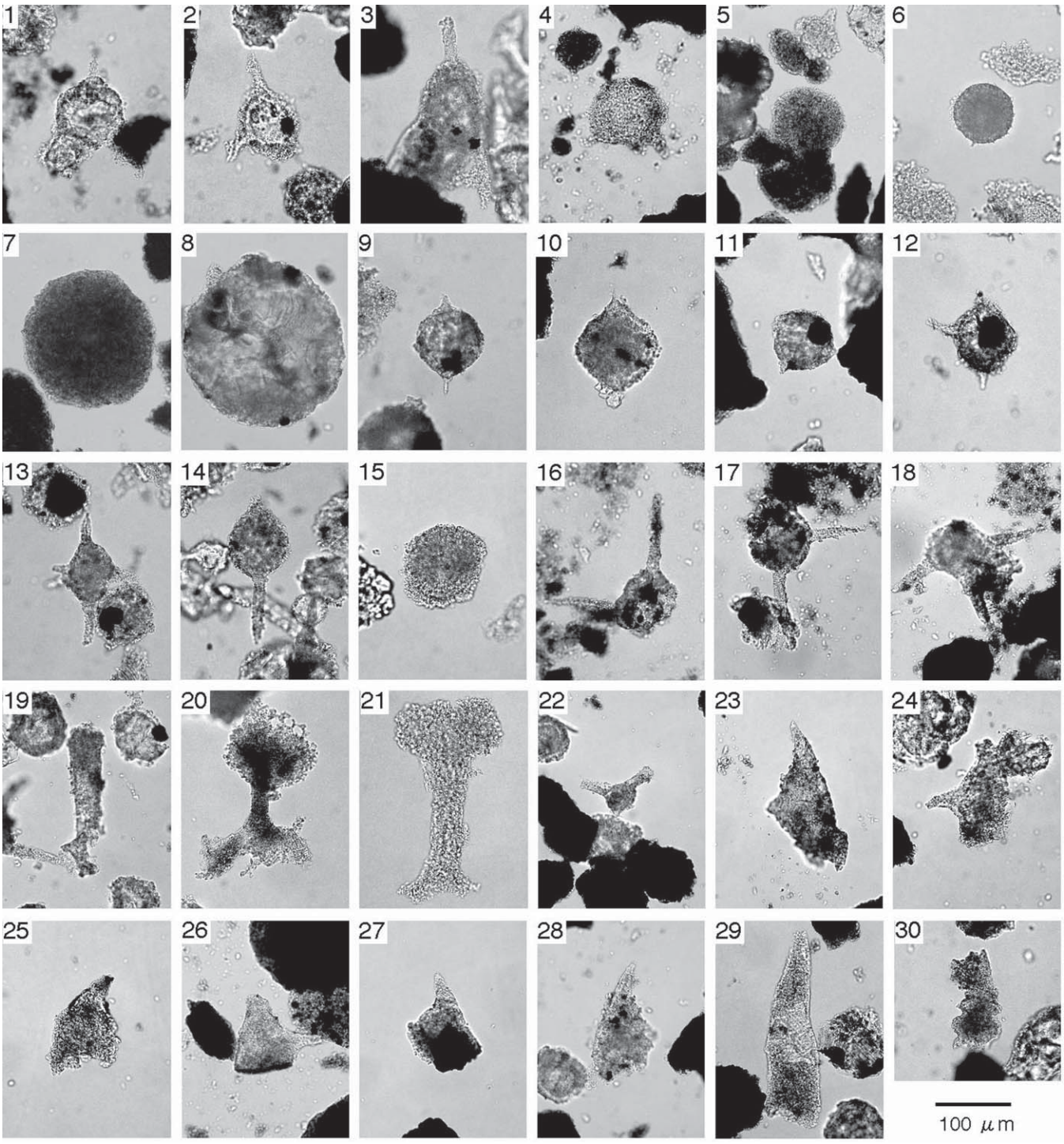

Figure 11. Triassic radiolarians and enigmatic Permian radiolarians extracted from the chert intercalated in the upper unit of section NF 1212R. See Figure 8 for the stratigraphic levels of the samples. **1–4.** *Hozmadia* sp. 1–3: NF1212k, 4: NF1212R-55. **5–6.** Sphaeroid A. 5: NF1212q, 6: NF1212R-53. **7–8.** Sphaeroid B. 7: NF1212q, 8: NF1212R-53. **9–10.** Sphaeroid C, NF1212k. **11.** Sphaeroid D, NF1212R-53. **12.** Sphaeroid E, NF1212R-53. **13.** Sphaeroid F, NF1212k. **14.** *Archaeospongoprunum* sp., NF1212k. **15.** *Copicyntroides* sp., NF1212R-53. **16–18.** *Stigmosphaerostylus* sp., NF1212k. **19.** *Cauletella* sp., NF1212k. **20–21.** *Ishigaum* sp., NF1212R-53. **22.** *Pseudotormentus* sp., NF1212k. **23–28.** *Albaillella* spp., 23: NF1212R-53, 24–25: NF1212k, 26: NF1212R-54, 27–28: NF1212s. **29.** *Follicucullus*? sp., NF1212R-53. **30.** *Albaillella*? sp., NF1212k.

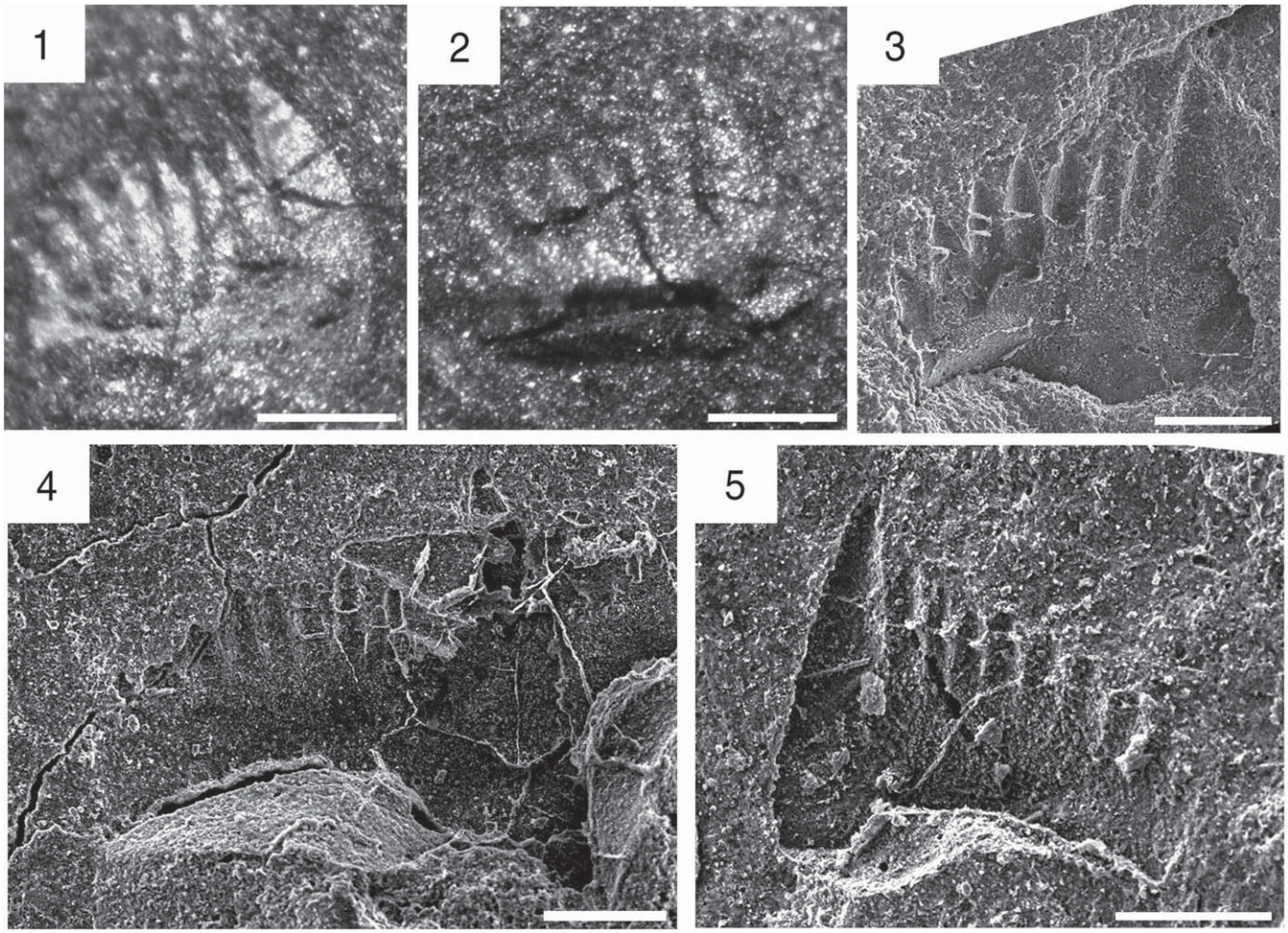

Figure 12. Early Triassic conodonts found in black claystone samples of the upper unit of section NF 1212R. See Figure 8 for the stratigraphic levels of the samples. **1–3.** *Hindeodus parvus* (Kozur and Pjatakova). 1: NF1212R-52, P_1 element, 2–3: NF1212R-q, P_1 element. **4–5.** *Hindeodus typicalis* (Sweet). NF1212R-q, P_1 element. All scale bars=100 μm. 1–2: stereo microscopic views; 3–5: scanning electron microscopic views.

Comparison with previously reported PTB siliceous rocks

PTB siliceous rocks have been reported from several sections in the Jurassic accretionary terranes of Japan (Nakaoi: Yamakita, 1988; Tenjinmaru: Yamakita, 1987; Kuwahara and Yamakita, 2001; Fujioka: Ishida *et al.*, 1992; Ubara: Kuwahara *et al.*, 1991; Yamakita *et al.*, 1999; Nabejiriyama: Ishiga *et al.*, 1982; Kuwahara, 1997; Koike *et al.*, 2004; Gujo-hachiman: Kuwahara *et al.*, 1998; Kuwahara and Yao, 2001; Akkamori: Takahashi *et al.*, 2009), and from New Zealand (Arrow Rocks: Aita and Spörli, 2007). Some of these sections are inadequate for comparison, chiefly because of the poor age control and disruption of stratigraphic continuity. We chose three PTB siliceous-rock sections for comparison with the NF 1212R section. Chosen for comparison are the Ubara, Gujo-hachiman, and Akkamori sections (Figure 13). The NF 1212R section is basically similar in stratigraphy, lithology, and stratigraphic position of the PTB to these PTB siliceous rocks, but also displays some dissimilarity.

Lithostratigraphy

No coarse-grained terrigenous clastic grains and beds occur in the four PTB siliceous-rock successions (Figure 13). Also, they commonly lack intercalations of tuffaceous beds. These common characteristics imply that these PTB siliceous rocks accumulated in a pelagic realm far beyond the reach of land-derived clastic and volcanic materials within the Panthalassa Ocean. The PTB siliceous-rock successions other than the four sections are also considered to have accumulated in a mid-Panthalassan pelagic setting without inputs of terrigenous and volcanic sediments.

The PTB siliceous-rocks successions of the Ubara, Gujo-

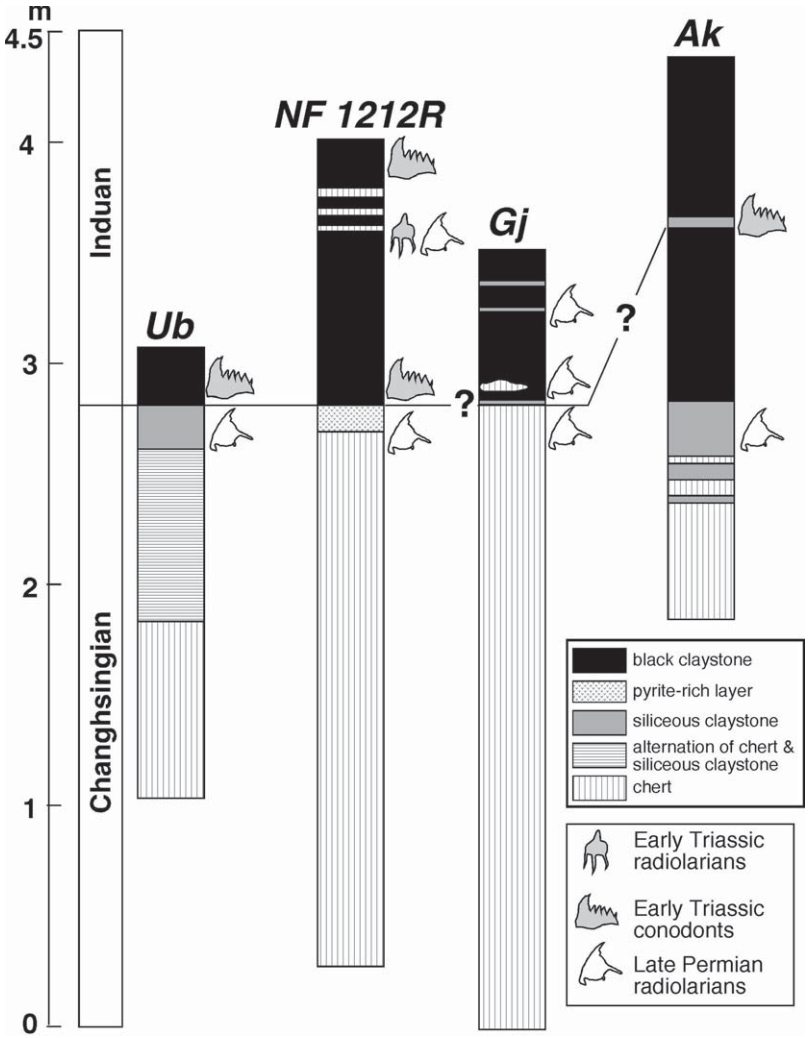

Figure 13. Stratigraphic comparison of the PTB siliceous rocks of section NF 1212R (this study) with Ubara, Gujo-hachiman, and Akkamori sections. Abbreviations Ub, Gj, and Ak stand for Ubara, Gujo-hachiman, and Akkamori sections, respectively.

hachiman, Akkamori, and NF 1212R sections commonly include a sharp lithologic transition from the siliceous rocks chiefly of chert with subordinate siliceous claystone to the overlying black claystone with minor intercalations of chert and siliceous claystone (Figure 13). The sharp facies transition means a sudden termination of the accumulation of siliceous sediments, which is, in turn, followed by an abrupt onset of dominant deposition of clayey sediments, reflecting a drastic change in paleoenvironmental conditions during the PTB interval. The sharp facies change corresponds with the stratigraphic level of the PTB in the Ubara and NF 1212R sections, and is recognized immediately above the highest occurrence of late Late Permian radiolarians in the Akkamori section.

The uppermost Permian chert of the four PTB siliceous-rocks sections is commonly bedded with clayey partings and alternating with siliceous claystone (Figure 13). The clayey sediments within the uppermost Permian chert units tend to slightly increase up-section towards the PTB. For instance, the chert grades up into an alternation of chert and siliceous claystone, which is followed by siliceous claystone at the top of the uppermost Permian siliceous rock succession at Ubara. A similar lithostratigraphic change is recorded also in the Akkamori section. The middle unit of section NF 1212R exhibits an upward increase in the thickness of the black clayey partings. Also, Algeo *et al.* (2010) showed a slight upward increase and sharp rise of the clay content in the upper Upper Permian chert and overlying black claystone, respectively, in the Gujo-hachiman section. The gradual upward increase of the clayey sediment in the uppermost Permian chert units represents a slight, gradual upward decline in the accumulation of radiolarian tests towards the end Permian, which

in turn, preceded a sudden onset of dominant deposition of clayey sediments.

Black claystone units of the Gujo-hachiman, Akkamori, and NF 1212R sections have thin, intermittent beds and lenses of chert and siliceous claystone (Figure 13). Also, a thin bed of siliceous claystone is recognized in the black claystone at Ubara. These siliceous rocks in the black claystone units are commonly gray, dark gray and black and rich in radiolarian remains and carbonaceous material. Intercalation of the radiolarians-bearing siliceous rocks in the black claystone units implies an intermittent and short-lived recovery of the supply of radiolarian tests immediately after the beginning of the Triassic.

Stratigraphic position of the PTB

The PTB of the Ubara, Akkamori, and NF 1212R sections is positioned on the basis of the first occurrence of *Hindeodus parvus,* which is indicative of the lowest Lower Triassic, and the last occurrence of radiolarians diagnostic of the upper Upper Permian *Neoalbaillella optima* Zone (Figure 13). As no reliable fossils indicative of the earliest Triassic are detected from the Gujo-hachiman section, the exact position of the PTB in it remains uncertain.

The biostratigraphically constrained PTB corresponds to a sharp lithologic boundary between the upper Upper Permian siliceous rocks and basal Triassic black claystone in the Ubara and NF 1212R sections. On the other hand, as the lowest occurrence of *H. parvus* is several tens of centimeters above the top of the uppermost siliceous claystone in the Akkamori section, the PTB there is positioned within the black claystone (Figure 13). Differing from Ubara and section NF 1212R, the Akkamori section records the latest Permian sedimentation of the black claystone (Takahashi *et al.*, 2009).

Summary

We described the lithostratigraphy and age of the PTB siliceous rocks within the Mino terrane, a representative Jurassic accretionary complex of Japan. Examined are an intact succession (section NF 1212R) and two reference sections (NF 1036R and NF 1207) of the Hashikadani Formation in the Mt. Funabuseyama area of the western part of the Mino Massif, central Japan.

The intact siliceous rock succession of section NF 1212R comprises a lower unit (ca. 1.7 m thick) of gray chert, a middle unit (ca. 0.9 m) of black to dark gray chert with a pyrite-rich layer at the top (ca. 0.1 m), and an upper unit (ca. 1.2 m) of black claystone with intermittent, thin beds of dark gray to black chert in ascending order. The chert of the lower and middle units is rich in radiolarian remains with minor siliceous sponge spicules. The upper part of the middle unit consists of carbonaceous black chert including tiny pyrite grains. The black claystone consists of cryptocrystalline quartz and clay minerals with a great admixture of carbonaceous matter, and contains a minor amount of flattened radiolarian remains. The black chert intercalated in the upper unit is also carbonaceous and rich in radiolarian remains. The lower and middle units are correlated with the *Neoalbaillella optima* Zone (Changhsingian). The basal 15-cm-thick part of the upper unit is referable to the *Hindeodus parvus* Zone (lowest Lower Triassic), and the overlying part is possibly correlated with the middle to upper Dienerian. We accurately position the PTB at the clearly defined base of the upper unit.

Measured PTB siliceous rocks are attributed to the upper part of the Hashikadani Formation, reconstructed as a Lower Permian to Lower Triassic deep-marine chert-dominant unit resting upon the lower flank of a seamount in a mid-oceanic realm of the Panthalassa Ocean. Our results present the world's first example of deep-marine PTB siliceous rocks associated with a Panthalassic seamount.

The PTB siliceous rocks of NF 1212R and the Ubara, Gujo-hachiman, and Akkamori sections are commonly characterized by a sharp lithologic change from chert to black claystone across the PTB transition. The biostratigraphically controlled PTB corresponds with this sharp lithologic boundary in the Ubara and NF 1212R sections. As the lowest occurrence of *H. parvus* is several tens of centimeters higher than the top of the uppermost siliceous claystone in the Akkamori section, the PTB there is positioned within the black claystone.

The sharp facies change common in the four PTB siliceous-rock sections implies a sudden cessation of the accumulation of siliceous sediments, which is, in turn, followed by an abrupt onset of dominant deposition of clayey sediments, presumably controlled by a drastic change in paleoenvironmental conditions across the PTB transition. The dominant deposition of clayey sediments is preceded by a slight and gradual rise of the clayey sedimentation nearly at the end of the Permian. The black claystone units of the four sections commonly have thin, intermittent beds of radiolarian chert and siliceous claystone. Their intercalation records an intermittent and short-lived recovery of the supply of radiolarian tests immediately after the beginning of the Triassic.

Acknowledgments

Special thanks are due to Neo Kaihatsu Limited Company (Neo, Gifu Prefecture) for permitting fieldwork along the logging road on the Amanokawara plateau. The authors express sincere thanks to Sayo Ukon and Atsushi Takano, who polished thin sections of the PTB siliceous rocks. We thank Katsuo Sashida and an anonymous reviewer for their critical reviews of the manuscript and constructive suggestions.

References

Agematsu, S., Sano, H. and Sashida, K., 2010: Reconstruction of *Hindeodus* apparatuses, the earliest Triassic conodonts. *Abstracts with Programs, 2010 Annual Meeting of the Paleontological Society of Japan*, p. 46. (*in Japanese*)

Aita, Y. and Spörli, K. B., 2007: Geological framework for the pelagic Permian/Triassic oceanic sequence of Arrow Rocks, Waipapa Terrane, Northland. *In,* Spörli, K. B., Takemura, A. and Hori, R. S. *eds., The oceanic Permian/Triassic boundary sequence at Arrow Rocks (Oruatemanu), Northland, New Zealand.* GNS Science Monograph 24, p. 1–16.

Algeo, T. J., Hinnov, L., Moser, J., Maynard, J. B., Elswick, E., Kuwahara, K. and Sano, H., 2010: Changes in productivity and redox conditions in the Panthalassic Ocean during the latest Permian. *Geology*, vol. 38, p. 187–190.

Bond, D. P. G. and Wignall, P. B., 2010: Pyrite framboid study of marine Permian-Triassic boundary sections: A complex anoxic event and its relationship to contemporaneous mass extinction. *Bulletin of* the *Geological Society of America*, vol. 122, p. 1265–1279.

Bowring, S. A., Erwin, D. H., Jin, Y. G., Martin, M. W., Davidek, K. and Wang, W., 1998: U/Pb zircon geochronology and tempo of the end-Permian mass extinction. *Science*, vol. 280, p. 1039–1045.

Bragin, N. J., 1991: Radiolaria and Lower Mesozoic units of the USSR east regions. *Transactions of the Academy of Sciences of the USSR*, vol. 469, p. 1–125. (*in Russian with English summary*)

Cao, C., Love, G. D., Hays, L. E., Wang, W., Shen, S. and Summons, R. E., 2009: Biogeochemical evidence for euxinic oceans and ecological disturbance presaging the end-Permian mass extinction event. *Earth and Planetary Science Letters*, vol. 281, p. 188–201.

De Wever, P., Dumitrica, P., Caulet, J. P., Nigrini, C. and Caridroit, M., 2001: *Radiolarians in the Sedimentary Record*. 533 p. Gordon and Breach Science Publishers, Amsterdam.

De Wever, P., O'Dogherty, L. and Goričan, Š., 2006: The plankton turnover at the Permian-Triassic boundary, emphasis on radiolarians. *Eclogae Geologicae Helvetiae,* vol. 99, Supplement 1, S49–S62.

Dumitrica, P., Kozur, H. and Mostler, H., 1980: Contribution to the radiolarian fauna of the Middle Triassic of the Southern Alps. *Geologisch-palontologische Mitteilungen Innsbruck*, Bd. 10, p. 1–46.

Erwin, D. H., 2006: *Extinction: How Life on the Earth Nearly Ended,* 296 p. Princeton University Press, Princeton.

Feng, Q., He, W., Gu, S., Jin, Y. and Meng, Y., 2006a: Latest Permian Spumellaria and Entactinaria (Radiolaria) from South China. *Revue de Micropaléontologie*, vol. 49, p. 21–43.

Feng, Q., He, W., Gu, S., Meng, Y., Jin, Y. and Zhang, F., 2007: Radiolarian evolution during the latest Permian in South China. *Global and Planetary Changes*, vol. 55, p. 177–192.

Feng, Q., He, W., Zhang, S. and Gu, S., 2006b: Taxonomy of order Latentifistularia (Radiolaria) from the latest Permian in southern Guangxi, China. *Journal of Paleontology*, vol. 80, p. 826–848.

Feng, Q., Yang, F., Zhang, Z., Zhang, N., Gao, Y. and Wang, Z., 2000: Radiolarian evolution during the Permian and Triassic transition in south and southeast China. *In,* Yin, H., Dickins, J. M., Shi, G. R. and Tong, J. *eds.*, *Permian-Triassic Evolution of Tethys and Western Circum-Pacific*. p. 309–326. Elsevier, New York.

Feng, Q., Zhang, Z. and Ye, M., 2001: Middle Triassic radiolarian fauna from southwest Yunnan, China. *Micropaleontology*, vol. 47, p. 173–204.

Grasby, S. E. and Beauchamp, B., 2009: Latest Permian to Early Triassic basin-to shelf anoxia in the Sverdrup Basin, Arctic Canada. *Chemical Geology*, vol. 264, p. 232–246.

Ishida K., Yamashita M. and Ishiga, H., 1992: P/T boundary in pelagic sediments in the Tanba Belt, Southwest Japan. *Geological Reports of Shimane University*, vol. 11, p. 39–57. (*in Japanese*)

Ishiga, H., 1986: Late Carboniferous and Permian radiolarian biostratigraphy of Southwest Japan. *Journal of Geoscience, Osaka City University*, vol. 29, p. 89–100.

Ishiga. H., Kito, T. and Imoto, N., 1982: Late Permian radiolarian assemblages in the Tamba district and adjacent area, Southwest Japan. *Earth Science* (*Chikyu Kagaku*), vol. 36, p. 10–22.

Isozaki, Y., 1997a: Permo-Triassic boundary superanoxia and stratified super ocean: records from lost deep sea. *Science*, vol. 276, p. 235–238.

Isozaki, Y., 1997b: Jurassic accretion tectonics of Japan. *Island Arc*, vol. 6, p. 25–51.

Jiang, H., Lai, X., Luo, G., Aldridge, R., Zhang, K. and Wignall, P. B., 2007: Restudy of conodont zonation and evolution across the P/T boundary at Meishan section, Changxing, Zhejiang, China. *Global and Planetary Changes*, vol. 55, p. 39–55.

Jones, G., Valsami-Jones, E. and Sano, H., 1993: Nature and tectonic setting of accreted basalts from the Mino terrane, central Japan. *Journal of the Geological Society*, vol. 150, p. 1167–1181.

Kajiwara, Y., Yamakita, S., Ishida, K., Ishiga, H. and Imai, A., 1994: Development of a largely anoxic stratified ocean and its temporary massive mixing at the Permian/Triassic boundary supported by the sulfur isotope record. *Palaeogeography, Palaeoclimatology, Palaeoecology*, vol. 111, p. 367–379.

Kamata, Y., Matsuo, A., Takemura, A., Yamakita, S., Aita, Y., Sakai, T., Suzuki, N. and Hori, R. S., 2007: Late Induan (Dienerian) primitive nassellarians from Arrow Rocks, Northland, New Zealand. *In,* Spörli, K. B., Takemura, A. and Hori, R. S. *eds., The oceanic Permian/Triassic boundary sequence at Arrow Rocks (Oruatemanu), Northland, New Zealand.* GNS Science Monograph 24, p. 109–116.

Kauffman, E. G. and Erwin, D. H., 1995: Surviving mass extinction. *Geotimes,* vol. 40, p. 14–17.

Kiessling, W., Flügel, E. and Golonka, J., 1999: Paleoreef maps: Evaluation of a comprehensive database on Phanerozoic reefs. *Bulletin of the American Association of Petroleum Geologists,* vol. 83, p. 1552–1587.

Knoll, A. H., Bambach, R. K., Payne, J. L., Pruss, S. and Fischer, W. W., 2007: Paleophysiology and end-Permian mass extinction. *Earth and Planetary Science Letters*, vol. 256, p. 295–313.

Koike, T., Yamakita, S. and Kadota, N., 2004: A natural assemblage of *Ellisonia* sp. cf. *E. triassica* Müller (Vertebrata: Conodonta) from the uppermost Permian in the Suzuka Mountains, central Japan. *Paleontological Research*, vol. 8, p. 241–253.

Kojima, S., 1989: Mesozoic terrane accretion in northeast China, Sikhote-Alin and Japan regions. *Palaeogeography*, *Palaeoclimatology*, *Palaeoecology*, vol. 69, p. 213–232.

Korte, C., Jasper, T., Kozur, H. W. and Veizer, J., 2005: $\delta^{18}O$ and $\delta^{13}C$ of Permian brachiopods: A record of seawater evolution and continental glaciation. *Palaeogeography*, *Palaeoclimatology*, *Palaeoecology*, vol. 224, p. 333–351.

Korte, C. and Kozur, H. W., 2010: Carbon-isotope stratigraphy across the Permian-Triassic boundary: A review. *Journal of Asian Earth Sciences*, vol. 39, p. 215–235.

Korte, C., Kozur, H. W., Joachimski, M. M., Strauss, H., Veizer, J. and Schwark, L., 2004: Carbon, sulfur, oxygen and strontium isotope records, organic geochemistry and biostratigraphy across the Permian/Triassic boundary in Abadeh, Iran. *International Journal of Earth Sciences* (*Geologische Rundschau*), vol. 93, p. 565–581.

Kozur, H. W., 1998: Some aspects of the Permian–Triassic boundary (PTB) and of the possible causes for the biotic crisis around this boundary. *Palaeogeography, Palaeoclimatology, Palaeoecology*, vol. 143, p. 227–272.

Kuwahara K., 1997, Upper Permian radiolarian biostratigraphy: Abundance zones of *Albaillella. News of Osaka Micropaleontologists, Special Volume*, no. 10, p. 55–75. (*in Japanese*)

Kuwahara, K., Nakae, S. and Yao, A., 1991: Late Permian "Toishi-type" siliceous mudstone in the Mino-Tamba Belt. *Journal of the Geological Society of Japan*, vol. 97, p. 1005–1008. (*in Japanese*)

Kuwahara, K., Sano, H., Ezaki, Y. and Yao, A., 2010: Discovery of Triassic siliceous rocks from large Permian oceanic-rock mass in the Mt. Funabuseyama area of the western part of Mino terrane and its geologic implication. *The Journal of the Geological Society of Japan*, vol. 116, p. 321–340. (*in Japanese*)

Kuwahara K. and Yamakita S., 2001: Microbiostratigraphy on chert facies of Upper Permian in the Northern Chichibu Belt, Shikoku, Southwest

Japan. *News of Osaka Micropaleontologists, Special Volume*, no. 12, p. 51–59. (*in Japanese*)

Kuwahara K. and Yao, A., 2001: Late Permian radiolarian faunal change in bedded chert of the Mino Belt, Japan. *News of Osaka Micropaleontologists, Special Volume*, no. 12, p. 33–49. (*in Japanese*)

Kuwahara, K., Yao, A. and Yamakita, S., 1998: Reexamination of Upper Permian radiolarian biostratigraphy. *Earth Science* (*Chikyu Kagaku*), vol. 52, p. 391–404.

Lai, X., Wignall, P. B. and Zhang, K., 2001: Paleoecology of the conodonts *Hindeodus* and *Clarkina* during the Permian-Triassic transitional period. *Palaeogeography, Palaeoclimatology, Palaeoecology*, vol. 171, p. 63–72.

Lehrmann, D. J., Payne, J. L., Pei, D., Enos, P., Druke, D., Steffen, K., Zhang, J., Wei, J., Orchard, M. J. and Ellwood, B., 2007: Record of the end-Permian extinction and Triassic recovery in the Chongzuo-Pingguo platform, southern Nanpanjiang basin, Guangxi, south China. *Palaeogeography, Palaeoclimatology, Palaeoecology*, vol. 252, p. 200–217.

Lindström, S. and McLaughlin, S., 2007: Synchronous palynofloristic extinction and recovery after the end-Permian event in the Prince Charles Mountains, Antarctica: Implications for palynofloristic turnover across Gondwana. *Review of Palaeobotany and Palynology*, vol. 145, p. 89–122.

Matsuda, T. and Isozaki, Y., 1991: Well-documented travel history of Mesozoic pelagic chert in Japan: From remote ocean to subduction zone. *Tectonics*, vol. 10, p. 475–499.

Mizutani, S., 1990: Mino Terrane. *In,* Ichikawa, K., Mizutani, S., Hada, S. and Yao, A. *eds.*, *Pre-Cretaceous Terranes of Japan*, p. 121–135. Publication of International Geological Correlation Project #224, Osaka.

Monger, J. W. H., Wheeler, J. O., Tipper, H. W., Gabrielse, H., Harms, T., Struik, L. C., Campbell, R. B., Dodds, C. J., Gehrels, G. E. and O'Brien, J., 1991: Part B. Cordilleran terranes. *In,* Gabrielse, H. and Yorath, C. J. *eds.*, *Geology of the Cordilleran Orogen in Canada*, *Geology of Canada*, no. 4, p. 281–327. Geological Survey of Canada, Ottawa.

Nakae, S., 2000: Regional correlation of the Jurassic accretionary complex in the Inner Zone of Southwest Japan. *Memoirs of the Geological Society of Japan*, no. 55, p. 73–98.

Nielsen, J. K. and Shen, Y., 2004: Evidence for sulfidic deep water during the Late Permian in the East Greenland Basin. *Geology*, vol. 32, p. 1037–1040.

Orchard, M. J., 2007: Conodont diversity and evolution through the latest Permian and Early Triassic upheavals. *Palaeogeography, Palaeoclimatology, Palaeoecology*, vol. 252, p. 93–117.

Orchard, M. J., Cordey, F., Rui, L., Bamber, E. W., Mamet, B., Struik, L. C., Sano, H. and Taylor, H. J., 2001: Biostratigraphic and biogeographic constraints on the Carboniferous to Jurassic Cache Creek Terrane in central British Columbia. *Canadian Journal of Earth Sciences*, vol. 38, p. 551–578.

Orchard, M. J. and Krystyn, L., 1998: Conodonts of the lowermost Triassic of Spiti, and new zonation based on *Neogondolella* successions. *Rivista Italiana di Paleontologia e Stratigrafia,* vol. 104, p. 341–368.

Payne, J. L., Lehrmann, D. J., Wei, J., Orchard, M. J., Schrag, D. P. and Knoll, A. H., 2004: Large perturbations of the carbon cycle during recovery from the end-Permian extinction. *Science*, vol. 305, p. 506–509.

Pruss, S. B., Bottjer, D. J., Corsetti, F. A. and Baud, A., 2006: A global marine sedimentary response to the end-Permian extinction: Examples from southern Turkey and the western United States. *Earth-Science Reviews*, vol. 78, p. 193–206.

Sano, H., 1988: Permian oceanic-rocks of Mino terrane, central Japan. Part I. Chert facies. *The Journal of the Geological Society of Japan*, vol. 94, p. 697–709.

Sano, H. and Kojima, S., 2000: Carboniferous to Jurassic oceanic rocks of Mino-Tamba-Ashio terrane. *Memoirs of the Geological Society of Japan*, no. 55, p. 123–144. (*in Japanese*)

Sano, H., Kuwahara, K., Yao, A. and Agematsu, S., 2010: Permian-Triassic boundary siliceous rocks succession discovered in Iwaidani valley of the Funabuseyama area, western Mino terrane. *Abstracts with Programs, 2010 Annual Meeting of the Paleontological Society of Japan*, p. 48. (*in Japanese*)

Sano, H., Yamagata, T. and Horibo, K., 1992: Tectonostratigraphy of Mino terrane: Jurassic accretionary complex of southwest Japan. *Palaeogeography Palaeoclimatology Palaeoecology*, vol. 96, p. 41–57.

Sashida, K., Sardsud, A., Igo, H., Nakornsri, N., Adachi, S. and Ueno, K., 1998: Occurrence of Dienerian (Lower Triassic) radiolarians from the Phatthalung area of peninsular Thailand and radiolarian biostratigraphy around the Permian/Triassic boundary. *News of Osaka Micropaleontologists, Special Volume*, no. 11, p. 59–70. (*in Japanese*)

Sepkoski, J. J. Jr., 1984: A kinematic model of Phanerozoic taxonomic diversity. III. Post-Paleozoic families and mass extinction. *Paleobiology*, vol. 10, p. 246–267.

Sugiyama, K., 1992: Lower and Middle Triassic radiolarians from Mt. Kinkazan, Gifu Prefecture, central Japan. *Transactions and Proceedings of the Palaeontological Society of Japan, New Series*, no. 167, p. 1180–1223.

Sugiyama, K., 1997: Triassic and Lower Jurassic radiolarian biostratigraphy in the siliceous claystone and bedded chert units of the southeastern Mino Terrane, Central Japan. *Bulletin of the Mizunami Fossil Museum,* no. 24, p. 79–193.

Sweet, W. C., Mosher, L. C., Clark, D. L., Collinson, J. W. and Hasenmueller, W. C., 1971: Conodont biostratigraphy of the Triassic. *In,* Sweet, W. C. and Bergström, S. M. *eds.*, *Symposium on Conodont Biostratigraphy. Memoirs of the Geological Society of America,* no. 127, p. 441–465.

Takahashi, S., Kaiho, K., Oba, M. and Kakegawa, T., 2010: A smooth negative shift of organic carbon isotope ratios at an end-Permian mass extinction horizon in central pelagic Panthalassa. *Palaeogeography, Palaeoclimatology, Palaeoecology*, vol. 292, p.532–539.

Takahashi, S., Yamakita, S., Suzuki, N., Kaiho, K. and Ehiro, M., 2009: High organic carbon content and a decrease in radiolarians at the end of the Permian in a newly discovered continuous pelagic section: A coincidence? *Palaeogeography, Palaeoclimatology, Palaeoecology*, vol. 271, p. 1–12.

Takemura, A., Aita, Y., Hori, R. S., Higuchi, Y., Spörli, Campbell, H. J., Kodama, K. and Sakai, T., 2002: Triassic radiolarians from the ocean-floor sequence of the Waipapa Terrane at Arrow Rocks, Northland, New Zealand. *New Zealand Journal of Geology and Geophysics*, vol. 45, p. 289–296.

Takemura, A., Sakai, M., Sakamoto, S., Aono, R., Takemura, S. and Yamakita, S., 2007: Earliest Triassic radiolarians from the ARH and ARF sections on Arrow Rocks, Waipapa Terrane, Northland, New Zealand. *In,* Spörli, K. B., Takemura, A. and Hori, R. S. *eds., The oceanic Permian/Triassic boundary sequence at Arrow Rocks (Oruatemanu), Northland, New Zealand*. GNS Science Monograph 24, p. 97–107.

Takeuchi, M., 2000: Origin of Jurassic coarse clastic sediments in the Mino-Tanba Belt. *Memoirs of the Geological Society of Japan*, no. 55, p. 107–121.

Wakita, K., 1988: Origin of chaotically mixed rock bodies in the Early Jurassic to Early Cretaceous sedimentary complex of the Mino terrane, central Japan. *Bulletin of the Geological Survey of Japan*, vol. 39, p. 675–757.

Wignall, P. B., Bond, D. P. G., Kuwahara, K., Kakuwa, Y., Newton, R. J. and Poulton, S. W., 2010: An 80 million year oceanic redox history from Permian to Jurassic pelagic sediments of the Mino-Tamba terrane, SW Japan, and the origin of four mass extinctions. *Global and Planetary Changes*, vol. 71, p. 109–123.

Wignall, P. B. and Hallam, A., 1992: Anoxia as a cause of the Permian/Triassic mass extinction: facies evidence from northern Italy and the western United States. *Palaeogeography, Palaeoclimatology, Palaeoecology*, vol. 93, p. 21–46.

Wignall, P. B., Newton, R. and Brookfield, M. E., 2005: Pyrite framboid evidence for oxygen poor deposition during the Permian-Triassic crisis in Kashmir. *Palaeogeography, Palaeoclimatology, Palaeoecology*, vol. 216, p. 183–188.

Xia, W., Zhang, N., Kakuwa, Y. and Zhang, L., 2005: Radiolarian and conodont biozonation in the pelagic Guadalupian-Lopingian boundary interval at Dachongling, Guangxi, South China, and mid-upper Permian

global correlation. *Stratigraphy*, vol. 2, p. 217–238.

Yamakita, S., 1987: Stratigraphic relationship between Permian and Triassic strata of chert facies in the Chichibu Terrane in eastern Shikoku, *The Journal of the Geological Society of Japan*, vol. 93, p. 145–148.

Yamakita, S., 1988: Jurassic-earliest Cretaceous allochthonous complexes related to gravitational slidings in the Chichibu terrane in eastern and central Shikoku. southwest Japan. *Journal of the Faculty of Science, University of Tokyo, Section 2*, vol. 21, p. 467–514.

Yamakita, S., Kadota, N., Kato, T., Tada, R., Ogihara, S., Tajika, E. and Hamada, E., 1999: Confirmation of the Permian/Triassic boundary in deep sea sedimentary rocks; earliest Triassic conodonts from black carbonaceous claystone of the Ubara section in the Tamba Belt, Southwest Japan. *Journal of the Geological Society of Japan*, vol. 105, p. 895–898.

Yao, A., 2009: Spatio-temporal changes of Paleozoic-Mesozoic radiolarian faunas in Japan and paleoenvironmental changes. *Paleontological Research,* vol. 13, p. 45–52.

Yao, A. and Kuwahara, K., 1997: Radiolarian faunal change from Late Permian to Middle Triassic times. *News of Osaka Micropaleontologists, Special Volume*, no. 10, p. 87–96.

Yao, A., Kuwahara, K., Ezaki, Y., Liu, J., Hao, W., Luo, Y. and Kuang, G., 2005: Permian and Triassic radiolarians from the western Guangxi area, China. *Journal of Geoscience, Osaka City Univ*ersity, vol. 48, p. 81–93.

Yin, H., Zhang, K., Tong, J., Yang, Z. and Wu, S., 2001: The global stratotype section and point (GSGP) of the Permian-Triassic Boundary. *Episodes*, vol. 24, p. 102–114.

Zhao, L., Orchard, M. J., Tong, J., Sun, Z., Zuo, J., Zhang, S. and Yun, A., 2007: Lower Triassic conodont sequence in Chaofu, Anhui Province, China and its global correlation. *Palaeogeography, Palaeoclimatology, Palaeoecology*, vol. 252, p. 24–38.